Article

Ubiquitylation of lipopolysaccharide by RNF213 during bacterial infection

https://doi.org/10.1038/s41586-021-03566-4

Received: 27 November 2020

Accepted: 20 April 2021

Published online: 19 May 2021

Check for updates

Elsje G. Otten[1,4]✉, Emma Werner[1,4], Ana Crespillo-Casado[1], Keith B. Boyle[1], Vimisha Dharamdasani[1], Claudio Pathe[1], Balaji Santhanam[1,3] & Felix Randow[1,2]✉

Ubiquitylation is a widespread post-translational protein modification in eukaryotes and marks bacteria that invade the cytosol as cargo for antibacterial autophagy[1–3]. The identity of the ubiquitylated substrate on bacteria is unknown. Here we show that the ubiquitin coat on *Salmonella* that invade the cytosol is formed through the ubiquitylation of a non-proteinaceous substrate, the lipid A moiety of bacterial lipopolysaccharide (LPS), by the E3 ubiquitin ligase ring finger protein 213 (RNF213). RNF213 is a risk factor for moyamoya disease[4,5], which is a progressive stenosis of the supraclinoid internal carotid artery that causes stroke (especially in children)[6,7]. RNF213 restricts the proliferation of cytosolic *Salmonella* and is essential for the generation of the bacterial ubiquitin coat, both directly (through the ubiquitylation of LPS) and indirectly (through the recruitment of LUBAC, which is a downstream E3 ligase that adds M1-linked ubiquitin chains onto pre-existing ubiquitin coats[8]). In cells that lack RNF213, bacteria do not attract ubiquitin-dependent autophagy receptors or induce antibacterial autophagy. The ubiquitylation of LPS on *Salmonella* that invade the cytosol requires the dynein-like core of RNF213, but not its RING domain. Instead, ubiquitylation of LPS relies on an RZ finger in the E3 shell. We conclude that ubiquitylation extends beyond protein substrates and that ubiquitylation of LPS triggers cell-autonomous immunity, and we postulate that non-proteinaceous substances other than LPS may also become ubiquitylated.

The lifestyle of intracellular bacteria shields them from many canonical immune mechanisms, while exposing them to a variety of cell-autonomous defences that are unique to individual subcellular compartments[9]. Bacteria that attempt to colonize the cytosol are restricted in their ability to establish infections through selective macroautophagy (known as 'xenophagy')[3,10,11]. Xenophagy is directed towards two types of 'eat-me' signal that are associated with cytosol-invading bacteria: galectin 8 and poly-ubiquitin[2,10,12–14]. Galectin 8 is a cytosolic lectin that binds glycans that are exposed on damaged host membranes, and accumulates near cytosol-invading bacteria during their escape from phagosomes[12,15]. The ubiquitin coat associated with bacteria is generated by host E3 ubiquitin ligases that include LRSAM1[16], Parkin[17], LUBAC[8,18] and SMURF1[19], whose specific contributions to cell-autonomous immunity remain largely unknown. Of these, LUBAC requires pre-existing ubiquitin for its own recruitment, which indicates that a cascade of E3 enzymes generates and shapes the ubiquitin coat[8]. The ubiquitinome of infected cells includes bacterial outer membrane proteins, but whether the formation of the bacterial ubiquitin coat requires the ubiquitylation of specific bacterial substrates remains to be established[20,21].

We used structured illumination microscopy to study the ubiquitin coat of *Salmonella enterica* serovar Typhimurium (*S.* Typhimurium), which is a Gram-negative bacterium that causes gastroenteritis in humans. Upon invasion of host cells, *S.* Typhimurium resides in *Salmonella*-containing vacuoles, from which a fraction of bacteria escapes into the cytosol. We observed that, at 1 h after infection, poly-ubiquitin colocalized with galectin-8-positive remnants of *Salmonella*-containing vacuoles whereas at 4 h after infection (when galectin-8-positive membranes are no longer detected) poly-ubiquitin was associated with the bacterial surface (Fig. 1a). Bacteria therefore become sequentially associated with poly-ubiquitin that resides either on damaged host membranes or the bacterium itself. To characterize the ubiquitin on the bacterial surface, we isolated bacteria from infected cells at 4 h after infection (Fig. 1b). We immunoblotted with an antibody specific for conjugated ubiquitin (FK2), which revealed a ubiquitin smear above 50 kDa in wild-type bacteria; by contrast, the Δ*rfc* mutant of *S.* Typhimurium—which lacks the O-antigen polymerase that is required to synthesize smooth LPS[22] (Extended Data Fig. 1a)—carried distinct ubiquitylated products of low molecular weight, in addition to a faint ubiquitin smear above 100 kDa. The distinct banding pattern in *S.* Typhimurium Δ*rfc* revealed the existence of a prominent oligo-ubiquitylated substrate in the bacterial ubiquitin coat, which—as judged by the size of the smallest band (15 kDa)—has an apparent molecular weight of about 7 kDa. Ubiquitylation of LPS rather than a protein substrate explains the observed phenotypes: semi-rough LPS in *S.* Typhimurium Δ*rfc* has a matching molecular weight, and the variable length

[1]MRC Laboratory of Molecular Biology, Cambridge, UK. [2]Department of Medicine, Addenbrooke's Hospital, University of Cambridge, Cambridge, UK. [3]Present address: Department of Structural Biology and Center for Data Driven Discovery, St Jude Children's Research Hospital, Memphis, TN, USA. [4]These authors contributed equally: Elsje G. Otten, Emma Werner. ✉e-mail: gotten@mrc-lmb.cam.ac.uk; randow@mrc-lmb.cam.ac.uk

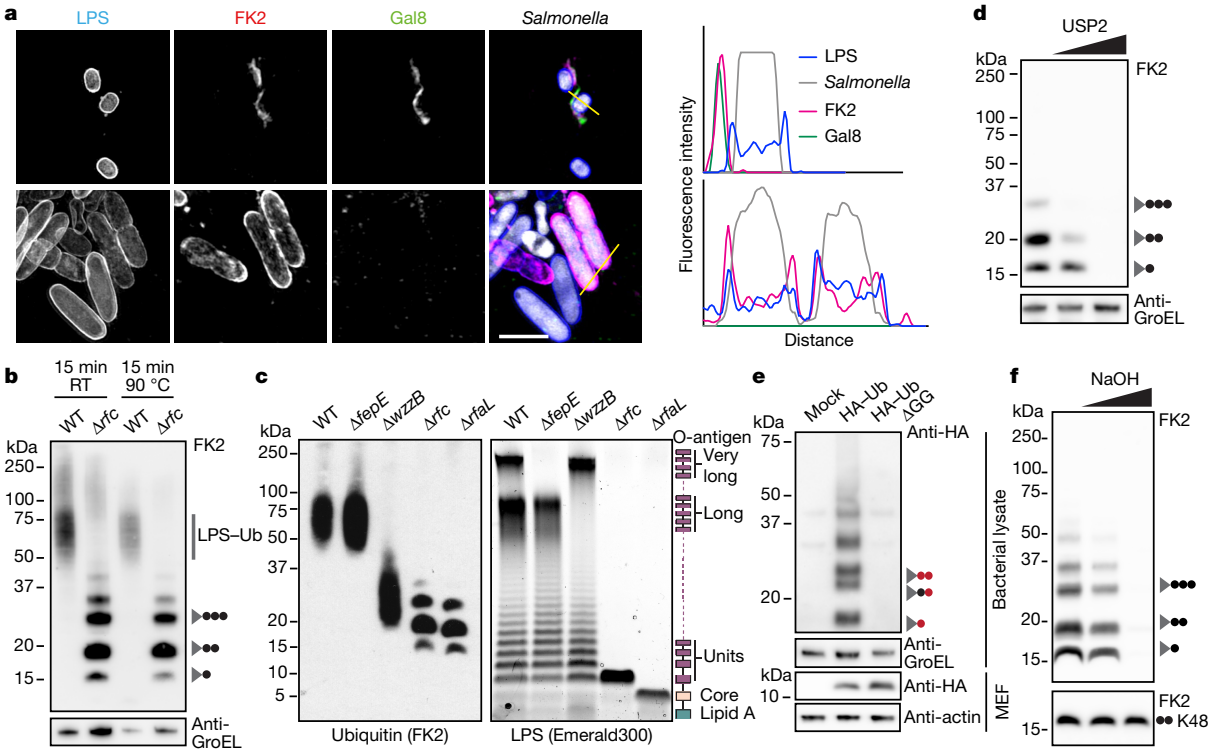

Fig. 1 | Ubiquitylation of LPS. a, Structured illumination micrograph of HeLa cells at 1 h after infection (top panels) and 4 h after infection (bottom panels) with *S.* Typhimurium, immunostained for LPS, FK2 and galectin 8 (Gal8). Scale bar, 3 µm. Lines indicate the plot profiles shown to the right. **b**–**f**, Immunoblot analysis of the indicated strains of *S.* Typhimurium, which were extracted from HeLa cells (**b**–**d**, **f**) or mouse embryonic fibroblasts (MEFs) stably expressing HA–ubiquitin or HA–ubiquitin(ΔGG) **(e)**. GroEL, loading control for bacterial lysates. Grey triangle, Δ*rfc* LPS; black circle, ubiquitin; red circle, HA–ubiquitin. RT, room temperature; WT, wild type. **b**, Bacterial lysates left at room temperature or incubated at 90 °C for 15 min. **c**, Right, Emerald300 stain of LPS extracted from the indicated *S.* Typhimurium strains grown in Luria broth. **d**, **f**, *S.* Typhimurium Δ*rfc* extracted from HeLa cells 4 h after infection and treated with 0 nM, 10 nM or 2 µM recombinant USP2 catalytic domain for 30 min (**d**) or lysed and incubated with 100 or 200 mM NaOH for 20 min (**f**). K48 Ub_2 was used as an amide-linked control. Representative of three biological repeats. For gel source data, see Supplementary Fig. 1.

of O-antigen chains in wild-type bacteria converts the ubiquitylated low-molecular-weight bands into a smear of higher molecular weight. To differentiate protein from non-protein ubiquitylation, we boiled bacterial lysates prepared in 'Bugbuster' (a lysis reagent that supports native protein conformation). The elimination of the ubiquitin smear of the highest molecular weight from both wild-type and mutant bacteria through boiling is indicative of protein ubiquitylation; by contrast, the distinct ubiquitin bands in *S.* Typhimurium Δ*rfc* and the majority of the ubiquitin smear in wild-type bacteria were heat-resistant, which is consistent with LPS ubiquitylation (Fig. 1b). To further verify the existence of ubiquitylated LPS, we generated additional *Salmonella* mutants deficient in distinct steps of LPS biosynthesis on the basis of our prediction that alterations in the LPS structure will cause corresponding changes in the ubiquitylation pattern (Fig. 1c). The Δ*rfaL* and Δ*rfc* mutants of *S.* Typhimurium—which are deficient in O-antigen ligase and polymerase, respectively—produced uniquely sized LPS that lacks all O-antigen or displays one O-antigen subunit only[22,23]. When isolated from cells, *S.* Typhimurium Δ*rfaL* and Δ*rfc* carried ubiquitylated products that accurately matched the size difference of their respective LPS. Wild-type bacteria produced O-antigens of three sizes: long chains and very long chains—the synthesis of which requires the regulators of O-antigen length WzzB and FepE, respectively—as well as shorter chains that are synthesized by the O-antigen polymerase Rfc when not engaged by WzzB[22,23]. In wild-type bacteria, LPS with very long O-antigen chains was not ubiquitylated. Thus, as predicted, the ubiquitylation of the Δ*fepE* mutant of *S.* Typhimurium was indistinguishable from that of wild-type bacteria. By contrast, the Δ*wzzB* mutant of *S.* Typhimurium, which lacks LPS with long O-antigen chains but still produces shorter chains through apo Rfc, carried ubiquitylated products of a correspondingly reduced size. To confirm the specificity of FK2 for ubiquitin, we (1) incubated *S.* Typhimurium Δ*rfc* extracted from cells with the deubiquitylating enzyme USP2, which depleted the characteristic ubiquitylated LPS pattern (Fig. 1d) and (2) isolated *S.* Typhimurium Δ*rfc* from cells that express HA-tagged ubiquitin, which reproduced the characteristic low-molecular-weight band pattern when probed with anti-HA antibody (Fig. 1e). Ubiquitin that lacks the C-terminal di-Gly motif was not conjugated. Taken together, our results demonstrate the ubiquitylation of LPS on cytosol-invading bacteria, a finding that extends the scope of ubiquitylation beyond a post-translational protein modification to an entirely different class of biomolecules.

Protein ubiquitylation targets primary amino or—occasionally—hydroxy groups, which results in amide- or ester-linked conjugates, respectively. The constitutive LPS core does not contain amino groups that are suitable for ubiquitylation (Extended Data Fig. 1a). However, substoichiometric modifications triggered by environmental cues can introduce such moieties in the form of 4-amino-L-arabinose or phosphoethanolamine. To test whether LPS ubiquitylation requires substoichiometric amino groups in the LPS core, we deleted *arnC* (which encodes the undecaprenyl-phosphate 4-deoxy-4-formamido-L-arabinose transferase that is required to generate 4-amino-L-arabinose) and the genes for the phosphoethanolamine transferases *eptA*, *eptB* and *cptA* from the Δ*rfaL* mutant of *S.* Typhimurium. Ubiquitylation of LPS proceeded unimpaired in individual mutants, as well as the pentuple knockout (*S.* Typhimurium *ΔrfaL ΔarnC ΔeptA ΔeptB ΔcptA*) (Extended Data Fig. 1a,b). We conclude that none of the known amino functions in LPS is required for its ubiquitylation. Ester-linked ubiquitin, in contrast to amide-linked conjugates, is sensitive to mild alkaline hydrolysis. We found that ubiquitylated

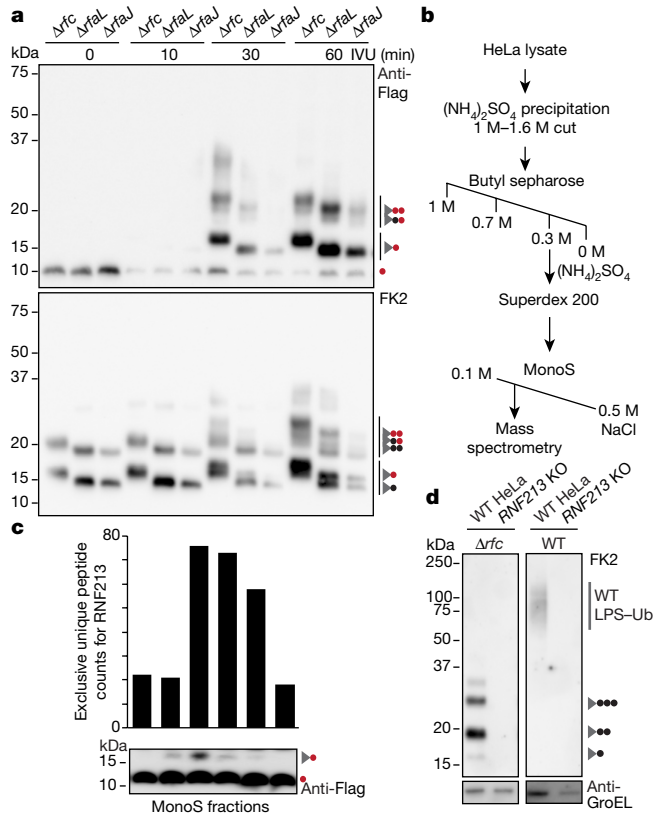

Fig. 2 | RNF213 is required for ubiquitylation of LPS. a, In vitro ubiquitylation (IVU) of the indicated *S*. Typhimurium strains extracted from infected HeLa cells. The in vitro ubiquitylation reaction comprised Flag–ubiquitin, E1 enzyme (UBE1), E2 enzyme (UBCH5C) and HeLa lysate as E3 ligase donor, and was terminated at the indicated time points. Red circle, Flag–ubiquitin; black circle, ubiquitin; grey triangle, LPS. **b**, Purification scheme for the LPS-ubiquitylating activity. **c**, In vitro ubiquitylation of Hela-extracted *S*. Typhimurium Δ*rfc* with fractions eluted from a MonoS column as E3 donor. Graph indicates the exclusive unique peptide count for RNF213 detected by mass spectrometry. Red circle, Flag–ubiquitin; grey triangle, Δ*rfc* LPS. **d**, Immunoblot analysis of the indicated *S*. Typhimurium strains extracted from wild-type and RNF213-knockout (KO) HeLa cells. Black circle, ubiquitin; grey triangle, Δ*rfc* LPS. In **a**, **c**, **d**, blots were probed with the indicated antibodies. In **a**–**c**, $n = 1$. **d**, Representative of three biological repeats. For gel and graph source data, see Supplementary Fig. 1 and Source Data.

LPS—but not the amide-linked ubiquitin that we used as a control—was hydrolysed under alkaline conditions (Fig. 1f), which further confirms that ubiquitylation of LPS does not proceed through amide linkage.

To reconstitute the ubiquitylation of LPS in vitro we incubated *S*. Typhimurium isolated from infected cells with recombinant E1 and E2 enzymes (UBE1 and UBCH5C, respectively), HeLa lysates as the source of E3 activity and Flag–ubiquitin. We used three strains of *S*. Typhimurium (Δ*rfc*, Δ*rfaL* and Δ*rfaJ*) that produce LPS of distinct sizes to unequivocally identify reaction products as ubiquitylated LPS (Extended Data Fig. 1a). Incubating the reaction for 30 min or longer produced mono- and oligo-ubiquitylated LPS (Fig. 2a). Mono-ubiquitylated LPS appeared as a singlet in anti-Flag and a doublet in FK2 blots owing to the size difference between Flag–ubiquitin–LPS synthesized in vitro and wild-type ubiquitin–LPS already present on bacteria extracted from cells. The generation of mono-Flag–ubiquitin–LPS indicates de novo ubiquitylation of LPS in vitro.

To identify the enzyme that generates mono-ubiquitylated LPS, we fractionated HeLa lysates by sequential ammonium sulfate precipitation, hydrophobic interaction chromatography, gel filtration and ion exchange chromatography, followed by mass spectrometry (Fig. 2b, Extended Data Fig. 2a). RNF213 was the only protein whose peptide counts matched the LPS ubiquitylating activity that eluted from the final column and that contained a domain characteristic of eukaryotic E3 ubiquitin ligases (that is, a RING, HECT or RBR domain) (Fig. 2c). To test whether RNF213 is required for the ubiquitylation of LPS, we used small interfering RNAs and CRISPR technology to deplete and knock out RNF213, respectively. Cells that lack RNF213 did not ubiquitylate LPS upon infection with wild-type or Δ*rfc S*. Typhimurium (Fig. 2d, Extended Data Fig. 2b–d), which reveals an essential role for RNF213 in ubiquitylating LPS on cytosol-invading bacteria in both human and mouse cells.

RNF213 is the largest recognized human E3 ligase, with a mass of almost 600 kDa. It features a large N-terminal disordered region followed by a stalk, a linker domain, a dynein-like core comprised of two catalytically active and four inactive AAA+ domains, and a C-terminal E3 module that surrounds the RING domain[24] (Fig. 3a, Extended Data Fig. 3a). *RNF213* is the major susceptibility gene for moyamoya disease, which is a cerebrovascular disorder that is characterized by bilateral stenosis of the supraclinoid internal carotid artery and abnormal formation of collateral vessels[4–7]. Moyamoya disease is caused by missense mutations in *RNF213* that are localized mainly to the domains surrounding the RING finger (the so-called E3 module). The physiological and pathophysiological role of RNF213 is not well understood: an involvement in lipotoxicity, lipid droplet formation, cell death and NF-κB signalling have all been reported[25–28].

To produce a structure–function analysis of RNF213, we complemented *Rnf213*-knockout mouse embryonic fibroblasts with human *RNF213* alleles (Fig. 3b). RNF213 remained active upon deletion of the N-terminal disordered region ($RNF213^{\Delta 1-586}$). Further N-terminal shortening ($RNF213^{\Delta 1-1009}$) prevented efficient ubiquitylation of LPS, as did a C-terminal truncation ($RNF213^{1-5186}$). To test the importance of the dynein-like core, we mutated the two catalytically active AAA+ domains in their Walker A and B motifs to disable ATP binding ($RNF213^{K2426A}$ and $RNF213^{K2775A}$) and hydrolysis ($RNF213^{E2488A}$ and $RNF213^{E2845A}$), respectively[24,28] (Fig. 3b). ATP binding by both domains was essential for efficient ubiquitylation of LPS, as was ATP hydrolysis by the fourth—but not the third—AAA+ domain. We next tested *RNF213* alleles from patients with moyamoya disease. None of the chosen alleles ($RNF213^{R4810K}$, $RNF213^{A5021V}$, $RNF213^{T4638I}$ and $RNF213^{E4950D}$) affected ubiquitylation of LPS (Fig. 3b). Finally, to test whether the RING domain mediates ubiquitylation of LPS, we introduced inactivating point mutations ($RNF213^{H4014N}$ or $RNF213^{W4024R}$). Neither mutation affected catalytic activity, nor did a deletion of the entire RING domain ($RNF213^{\Delta 3997-4036}$) (Fig. 3b). We conclude that RNF213-mediated ubiquitylation of LPS on cytosolic *S*. Typhimurium requires a catalytically active AAA+ module but is independent of the RING domain, consistent with a previous report of RING-independent autoubiquitylation of RNF213[24].

To fully reconstitute ubiquitylation of LPS in vitro, we purified recombinant RNF213 from *Spodoptera frugiperda* Sf9 cells (Extended Data Fig. 3b), which is a cell type with no endogenous LPS-ubiquitylating activity (Fig. 3c, Extended Data Fig. 3c). Purified RNF213 required the presence of ATP, as well as E1 and E2 enzymes, to ubiquitylate LPS on bacteria extracted from host cells, thus confirming a canonical mode of reaction (Fig. 3d, Extended Data Fig. 3d). Recombinant RNF213 also ubiquitylated purified rough LPS as well as lipid A, which confirms RNF213 as a bona fide LPS E3 ubiquitin ligase and reveals lipid A as its minimal substrate (Fig. 3e, Extended Data Fig. 1c). The site or sites of ubiquitylation in lipid A remain unknown. Consistent with hydrolysis of ubiquitylated LPS under mild alkaline conditions (Fig. 1f), RNF213-mediated ubiquitylation of lipid A may target hydroxy groups on either the sugars or fatty acids of lipid A, although ubiquitylation of the phosphate groups of lipid A is also conceivable. Taken together, we conclude that ubiquitylation of the lipid A moiety of LPS is mediated by RING-independent E3 ligase activity of RNF213.

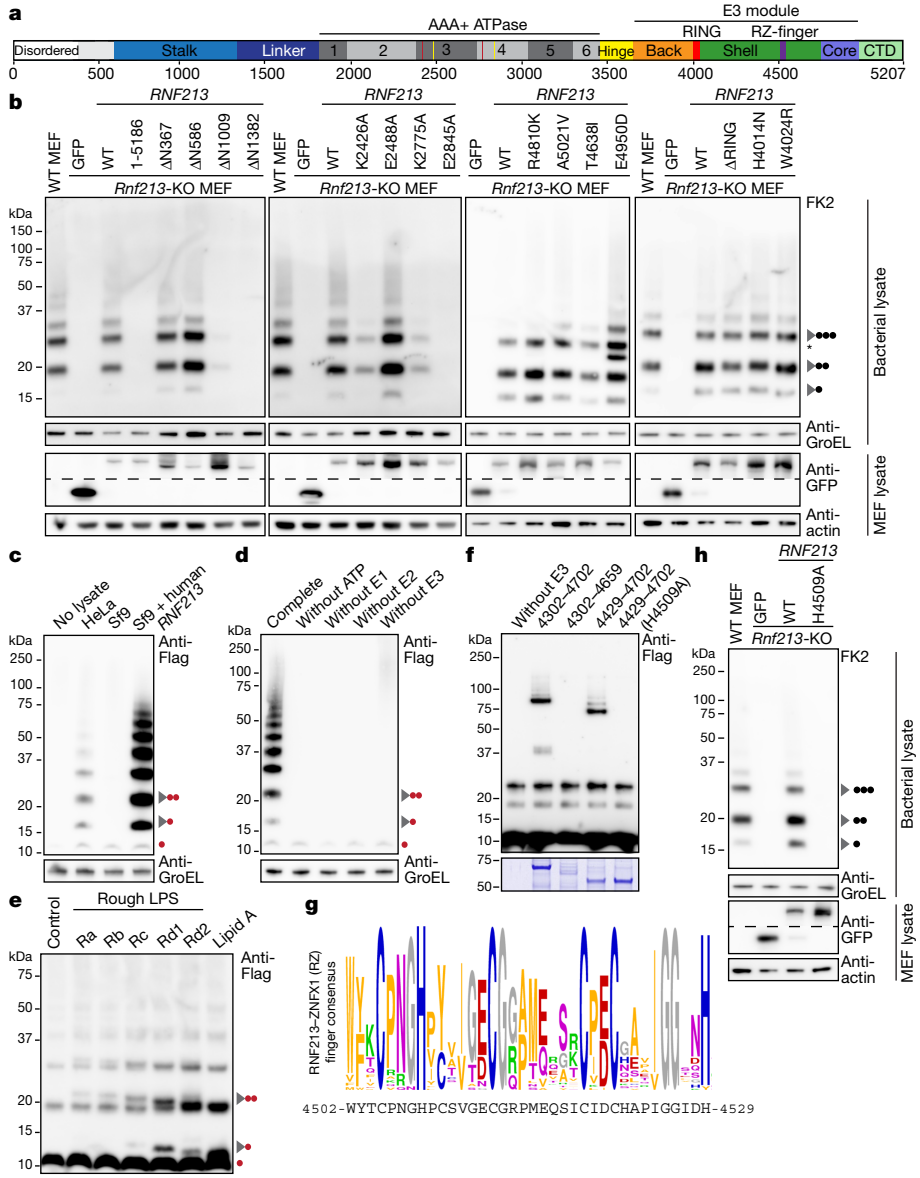

Fig. 3 | Ubiquitylation of LPS by RNF213 is a RING-independent, RZ-finger-mediated reaction. a, RNF213 domain structure. Critical residues in Walker A (K2426 and K2775) and Walker B motifs (E2488 and E2845) are indicated with red and yellow lines, respectively. CTD, C-terminal domain. **b**, **h**, immunoblot analysis of *S.* Typhimurium Δ*rfc* extracted from wild-type or *Rnf213*-knockout MEFs complemented with *GFP* or *GFP–RNF213* alleles as indicated. GFP blots present the upper and lower part of continuous blots from which the middle parts have been removed (as indicated by the dashed line). Black circle, ubiquitin; grey triangle, Δ*rfc* LPS. **c**–**e**, Immunoblot analysis of *S.* Typhimurium Δ*rfc* extracted from HeLa cells (**c**, **d**) or purified LPS from indicated *Salmonella enterica* ser. Minnesota strains (**e**) and subjected to in vitro ubiquitylation using HeLa, Sf9 or Sf9 cells expressing human *RNF213* lysates (**c**) or purified RNF213 (**d**, **e**). Red circle, Flag–ubiquitin; grey triangle, Δ*rfc* LPS (**c**, **d**) or LPS and lipid A (**e**). **f**, Immunoblot analysis of an in vitro ubiquitylation reaction using GST-tagged RNF213 fragments expressed in *E. coli* to assess autoubiquitylating activity. Representative of three experiments. **b**–**f**, **h**, Blots were probed with the indicated antibodies. Actin and GroEL were loading controls for mammalian and bacterial lysates, respectively. **g**, RZ finger consensus amongst RNF213 and ZNFX1 proteins; human RNF213 protein sequence is depicted below. In **b**, asterisk indicates a nonspecific band. Experiments in **b**, **d**–**f**, **h** are representative of at least three biological repeats. In **c**, $n = 1$ For gel source data, see Supplementary Fig. 1.

To identify the RNF213 domain that is required for RING-independent activity, we screened RNF213 fragments expressed in *Escherichia coli* for autoubiquitylating activity in vitro. RNF213(4302–4702) became mono- and oligo-ubiquitylated upon incubation with E1 (UBE1) and UBCH7, a *trans*-thiolating E2 enzyme that has previously been reported[24] to be the most active E2 for RNF213 (Fig. 3f). The activity of this fragment tolerated further N- but not C-terminal truncation, which reveals that RNF213(4430–4702) is the minimal active fragment. Neither fragment contained the RING domain. When mapped onto the structure of mouse RNF213, RNF213(4302–4702) comprised the middle and C-terminal lobes of the E3 shell; RNF213(4430–4702) comprised the C-terminal lobe only (Extended Data Fig. 3a). Although the C-terminal lobe of RNF213 is not homologous to other proteins, a unique 27-amino-acid peptide inserted into the C-terminal lobe has sequence similarity to the NFX1-type zinc finger containing protein (ZNFX1), which is an interferon-induced RNA helicase that has antiviral function[29] (Fig. 3g, Extended Data Fig. 3a, e). We therefore name this 27-amino-acid peptide the RNF213–ZNFX1 finger (RZ finger). The RZ finger is not resolved in the RNF213 structure[24]; it contains two conserved histidine residues and four conserved cysteine residues, which suggests that it may form a Zn^{2+} complex. We tested the functional importance of the CHC_3H motif by creating *RNF213*$^{4430–4702,H4509A}$ and full-length *RNF213*^{H4509A}, which lost the

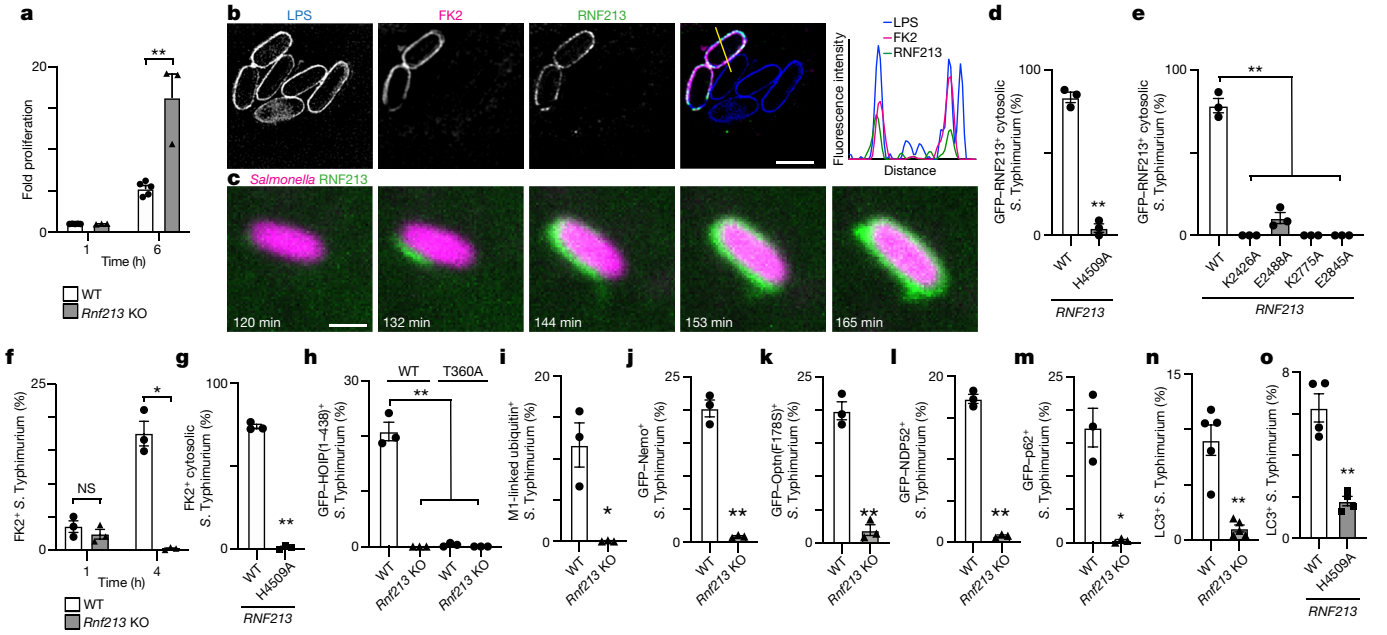

Fig. 4 | RNF213 provides cell-autonomous immunity. a, Fold replication of intracellular *S.* Typhimurium in wild-type and *Rnf213*-knockout MEFs, normalized to 1 h after infection time point. Bacteria were counted by serial dilution of cell lysate on Luria broth agar plates. **b**, Structured illumination micrograph of HeLa cells at 4 h after infection with *S.* Typhimurium and immunostained for LPS, ubiquitin (FK2) and RNF213. Scale bar, 3 µm. Line indicates the plot profile shown on the right. **c**, Still images from Supplementary Video 1. Instant structured illumination microscopy of MEFs expressing *Flag–GFP–RNF213* infected with *mCherry*-expressing *S.* Typhimurium. Times after infection are as indicated. Scale bar, 1 µm. **d**, **e**, Percentage of cytosolic *S.* Typhimurium positive for Flag–GFP–RNF213 at 3 h after infection. in wild-type or *Rnf213*-knockout MEFs stably expressing the indicated *GFP–RNF213* alleles. **f**–**o**, Percentage of *S.* Typhimurium positive at 3 h after infection for FK2 (ubiquitin) (**f**, **g**), GFP–HOIP(1–438) or GFP–HOIP(1–438, T360A) (**h**), M1-linked linear ubiquitin chains (**i**), GFP–Nemo (**j**), GFP–Optn(F178S) (**k**), GFP–NDP52 (**l**), GFP–p62 (**m**) and LC3 (**n**, **o**) in wild-type and *Rnf213*-knockout MEFs (**f**, **h**-**n**) or *Rnf213*-knockout MEFs stably expressing the indicated *GFP–RNF213* alleles (**g**, **o**). Statistical significance was assessed by two-tailed unpaired Student's *t*-test (**a**, **d**, **f**, **h**, **i**–**o**) or one-way analysis of variance (**e**, **h**). $^*P < 0.05$, $^{**}P < 0.01$. Data are mean ± s.e.m. of 3 (**a**–**m**),4 (**o**) or 5 (**n**) independent biological repeats.

ability to autoubiquitylate in vitro and to ubiquitylate LPS in infected cells, respectively (Fig. 3f, h). We conclude that the RZ finger presented by the C-terminal lobe of the E3 shell promotes autoubiquitylation and is essential for RNF213-mediated ubiquitylation of LPS similar to RING, HECT or RBR domains in other eukaryotic E3 ubiquitin ligases.

To test the functional importance of RNF213 for cell-autonomous immunity, we infected cells with *S.* Typhimurium. A lack of RNF213 had no effect on bacterial entry but cells that are deficient in RNF213 were impaired in restricting bacterial proliferation (Fig. 4a, Extended Data Fig. 4a). In wild-type cells, RNF213 was recruited to the surface of cytosolic *S.* Typhimurium, where it colocalized with ubiquitin (Fig. 4b). Instant structured illumination microscopy revealed that RNF213 recruitment started focally and subsequently spread around the bacterium, indicating cooperative behaviour (Fig. 4c, Supplementary Video 1). Recruitment of RNF213 to bacteria was not affected by *RNF213* alleles that are associated with moyamoya disease (*RNF213*^{R4810K}, *RNF213*^{A5021V}, *RNF213*^{T4638I} or *RNF213*^{E4950D}), but did require E3 ligase activity (as shown by the *RNF213*^{H4509A} allele) and a dynein-like core able to bind and hydrolyse ATP (as shown by the *RNF213*^{K2426A}, *RNF213*^{E2488A}, *RNF213*^{K2775A} and *RNF213*^{E2845A} mutants) (Fig. 4d, e, Extended Data Fig. 4b–e). The *RNF213*^{E2488A} mutant, which is deficient in ATP hydrolysis owing to a mutation in the Walker B motif of the third AAA+ domain, was impaired in forming a stable RNF213 coat (Fig. 4e, Extended Data Fig. 4e), despite efficiently ubiquitylating LPS on cytosolic bacteria (Fig. 3b). This phenotype reveals a specific requirement for the dynein-like AAA+ module in generating the RNF213 coat, possibly through effects on RNF213 oligomerization[28].

Cells that are deficient in RNF213 efficiently ubiquitylated remnants of *Salmonella*-containing vacuoles at 1 h after infection but did not create a ubiquitin coat on the surface of *S.* Typhimurium at 4 h after infection (Fig. 1a, 4f, Extended Data Fig. 4f), which reveals that ubiquitylated LPS is an essential component of the bacterial ubiquitin coat. Complementation with wild-type RNF213, but not with catalytically inactive *RNF213*^{H4509A}, restored the ubiquitin coat (Fig. 4g, Extended Data Fig. 4g). Deficiency in RNF213 curtailed recruitment of the LUBAC subunit HOIP (Fig. 4h, Extended Data Fig. 4h), as did inactivation of the ubiquitin-binding site in *HOIP*$^{1–438,T360A}$ (ref. [8]), which indicates that LUBAC recruitment requires RNF213-mediated ubiquitylation of LPS. Consequently, in the absence of RNF213, LUBAC did not add M1-linked ubiquitin chains to the bacterial ubiquitin coat (Fig. 4i, Extended Data Fig. 4i), which resulted in a failure to recruit Nemo (the M1-specific adaptor subunit of the IKK complex) (Fig. 4j, Extended Data Fig. 4j). The inability of RNF213-knockout cells to generate a bacterial ubiquitin coat at 4 h after infection abolished the recruitment of ubiquitin-binding autophagy cargo receptors—including LUBAC-dependent optineurin as well as LUBAC-independent NDP52 and p62[8] (Fig. 4k–m, Extended Data Fig. 4k–m)—and resulted in the failure of antibacterial autophagy, as indicated by the absence of LC3$^+$ *S.* Typhimurium (Fig. 4n, Extended Data Fig. 4n). Complementation with wild-type RNF213, but not with catalytically inactive *RNF213*^{H4509A}, restored the recruitment of LC3 to *S.* Typhimurium (Fig. 4o, Extended Data Fig. 4o). We conclude that RNF213 is essential for the generation of the bacterial ubiquitin coat and that cells lacking RNF213 suffer defects in cell-autonomous immunity that manifest as an inability to restrict the proliferation of *S.* Typhimurium (Extended Data Fig. 5).

The identification of RNF213 as an immune sensor reveals a link between moyamoya disease and infection. Although *RNF213* alleles that predispose individuals to moyamoya disease were not impaired

in their ability to ubiquitylate LPS, the activation of mutant RNF213 by bacterial or other infections may nevertheless contribute to the development of moyamoya disease in susceptible individuals. Activation during infection may explain the low penetrance of some risk alleles for moyamoya disease, such as *RNF213*^{R4810K}, which is an allele that is present in 16 million Asian individuals—of whom only 0.5% develop this disease[30]. Ubiquitylation of LPS by RNF213 requires ATPase activity in its dynein-like core. To access LPS embedded in bacterial membranes, the cytosolic LPS receptor caspase-4[31] also requires nucleotide hydrolysis, which is provided *in trans* by guanylate-binding proteins (GBPs)[32,33] (a family of interferon-induced GTPases). Nucleotide hydrolysis may thus represent a common requirement to sense LPS in cytosol-invading bacteria. Our discovery of the ubiquitylation of LPS expands the scope of ubiquitylation beyond that of a post-translational protein modification. Further non-proteinaceous ubiquitylation substrates may exist both in cytosol-invading pathogens and in host cells, which may be targeted by eukaryotic RING, HECT or RBR E3 ligases, by prokaryotic NEL or Sde E3 ligases or by unconventional E3 ligase activities that rely on novel domains, such as the RZ finger in the E3 shell of RNF213.

Online content

Any methods, additional references, Nature Research reporting summaries, source data, extended data, supplementary information, acknowledgements, peer review information; details of author contributions and competing interests; and statements of data and code availability are available at https://doi.org/10.1038/s41586-021-03566-4.

1. Huang, J. & Brumell, J. H. Bacteria–autophagy interplay: a battle for survival. *Nat. Rev. Microbiol.* **12**, 101–114 (2014).
2. Perrin, A. J., Jiang, X., Birmingham, C. L., So, N. S. Y. & Brumell, J. H. Recognition of bacteria in the cytosol of mammalian cells by the ubiquitin system. *Curr. Biol.* **14**, 806–811 (2004).
3. Deretic, V., Saitoh, T. & Akira, S. Autophagy in infection, inflammation and immunity. *Nat. Rev. Immunol.* **13**, 722–737 (2013).
4. Kamada, F. et al. A genome-wide association study identifies *RNF213* as the first moyamoya disease gene. *J. Hum. Genet.* **56**, 34–40 (2011).
5. Liu, W. et al. Identification of *RNF213* as a susceptibility gene for moyamoya disease and its possible role in vascular development. *PLoS ONE* **6**, e22542 (2011).
6. Scott, R. M. & Smith, E. R. Moyamoya disease and moyamoya syndrome. *N. Engl. J. Med.* **360**, 1226–1237 (2009).
7. Kuroda, S. & Houkin, K. Moyamoya disease: current concepts and future perspectives. *Lancet Neurol.* **7**, 1056–1066 (2008).
8. Noad, J. et al. LUBAC-synthesized linear ubiquitin chains restrict cytosol-invading bacteria by activating autophagy and NF-κB. *Nat. Microbiol.* **2**, 17063 (2017).
9. Schaible, U. E. & Haas, A. *Intracellular Niches of Microbe: A Pathogens Guide through the Host Cell* (Wiley Blackwell, 2009).
10. Birmingham, C. L., Smith, A. C., Bakowski, M. A., Yoshimori, T. & Brumell, J. H. Autophagy controls *Salmonella* infection in response to damage to the *Salmonella*-containing vacuole. *J. Biol. Chem.* **281**, 11374–11383 (2006).
11. Nakagawa, I. et al. Autophagy defends cells against invading group A *Streptococcus*. *Science* **306**, 1037–1040 (2004).
12. Thurston, T. L. M., Wandel, M. P., von Muhlinen, N., Foeglein, A. & Randow, F. Galectin 8 targets damaged vesicles for autophagy to defend cells against bacterial invasion. *Nature* **482**, 414–418 (2012).
13. Thurston, T. L. M., Ryzhakov, G., Bloor, S., von Muhlinen, N. & Randow, F. The TBK1 adaptor and autophagy receptor NDP52 restricts the proliferation of ubiquitin-coated bacteria. *Nat. Immunol.* **10**, 1215–1221 (2009).
14. Wild, P. et al. Phosphorylation of the autophagy receptor optineurin restricts *Salmonella* growth. *Science* **333**, 228–233 (2011).
15. Dupont, N. et al. *Shigella* phagocytic vacuolar membrane remnants participate in the cellular response to pathogen invasion and are regulated by autophagy. *Cell Host Microbe* **6**, 137–149 (2009).
16. Huett, A. et al. The LRR and RING domain protein LRSAM1 is an E3 ligase crucial for ubiquitin-dependent autophagy of intracellular *Salmonella* Typhimurium. *Cell Host Microbe* **12**, 778–790 (2012).
17. Manzanillo, P. S. et al. The ubiquitin ligase parkin mediates resistance to intracellular pathogens. *Nature* **501**, 512–516 (2013).
18. van Wijk, S. J. L. et al. Linear ubiquitination of cytosolic *Salmonella* Typhimurium activates NF-κB and restricts bacterial proliferation. *Nat. Microbiol.* **2**, 17066 (2017).
19. Franco, L. H. et al. The ubiquitin ligase Smurf1 functions in selective autophagy of *Mycobacterium tuberculosis* and anti-tuberculous host defense. *Cell Host Microbe* **21**, 59–72 (2017).
20. Fiskin, E., Bionda, T., Dikic, I. & Behrends, C. Global analysis of host and bacterial ubiquitinome in response to *Salmonella* Typhimurium infection. *Mol. Cell* **62**, 967–981 (2016).
21. Engström, P. et al. Evasion of autophagy mediated by *Rickettsia* surface protein OmpB is critical for virulence. *Nat. Microbiol.* **4**, 2538–2551 (2019).
22. Raetz, C. R. H. & Whitfield, C. Lipopolysaccharide endotoxins. *Annu. Rev. Biochem.* **71**, 635–700 (2002).
23. Whitfield, C. & Trent, M. S. Biosynthesis and export of bacterial lipopolysaccharides. *Annu. Rev. Biochem.* **83**, 99–128 (2014).
24. Ahel, J. et al. Moyamoya disease factor RNF213 is a giant E3 ligase with a dynein-like core and a distinct ubiquitin-transfer mechanism. *eLife* **9**, e56185 (2020).
25. Piccolis, M. et al. Probing the global cellular responses to lipotoxicity caused by saturated fatty acids. *Mol. Cell* **74**, 32–44.e8 (2019).
26. Sugihara, M. et al. The AAA+ ATPase/ubiquitin ligase mysterin stabilizes cytoplasmic lipid droplets. *J. Cell Biol.* **218**, 949–960 (2019).
27. Banh, R. S. et al. PTP1B controls non-mitochondrial oxygen consumption by regulating RNF213 to promote tumour survival during hypoxia. *Nat. Cell Biol.* **18**, 803–813 (2016).
28. Morito, D. et al. Moyamoya disease-associated protein mysterin/RNF213 is a novel AAA+ ATPase, which dynamically changes its oligomeric state. *Sci. Rep.* **4**, 4442 (2014).
29. Wang, Y. et al. Mitochondria-localised ZNFX1 functions as a dsRNA sensor to initiate antiviral responses through MAVS. *Nat. Cell Biol.* **21**, 1346–1356 (2019).
30. Liu, W., Hitomi, T., Kobayashi, H., Harada, K. H. & Koizumi, A. Distribution of moyamoya disease susceptibility polymorphism p.R4810K in RNF213 in East and Southeast Asian populations. *Neurol. Med. Chir. (Tokyo)* **52**, 299–303 (2012).
31. Shi, J. et al. Inflammatory caspases are innate immune receptors for intracellular LPS. *Nature* **514**, 187–192 (2014).
32. Wandel, M. P. et al. Guanylate-binding proteins convert cytosolic bacteria into caspase-4 signaling platforms. *Nat. Immunol.* **21**, 880–891 (2020).
33. Santos, J. C. et al. Human GBP1 binds LPS to initiate assembly of a caspase-4 activating platform on cytosolic bacteria. *Nat. Commun.* **11**, 3276 (2020).

Methods

No statistical methods were used to predetermine sample size. The experiments were not randomized, and investigators were not blinded to allocation during experiments and outcome assessment.

Plasmids, antibodies and chemicals

M6P plasmids were used to produce recombinant murine leukaemia viruses for the stable expression of proteins in mammalian cells[34]. pETM30 plasmids were used for protein expression in *E. coli*. To express *RNF213* in mammalian cells, an inducible PiggyBac transposon system was used[35]. *RNF213* cDNA was provided by D. Morito. To facilitate the generation of *RNF213* alleles, a codon-optimized *RNF213* cDNA was gene-synthesized (Genewiz). Mutations and gene truncations were generated by PCR using NEB HiFi and verified by sequencing.

The primary antibodies used were: FK2 (diluted 1:200, Enzo Life Science, BML-PW8810), anti-GroEL (1/1,000, Enzo Life Science, ADI-SPS-875-F), anti-DnaK (1:1,000, Enzo Life Science, ADI-SPA-880), anti-HA.11 (1:1,000, Convance, MMS-101R), anti-actin (1:1,000, Abcam, ab8227), anti-RNF213 (1:1,000, Merck, HPA003347), anti-Flag–M2–HRP (1:1,000, Merck, A8592) and anti-GFP (1:1,000, JL8, Clontech, 632381), anti-LPS (1:100, BioRad, 8210-0407), anti-galectin 8 (1:100, R&D Systems, AF1305), anti-M1 (1:1,000, 1F11/3F5/Y102L, GenenTech) and anti-LC3 (1:100, Cosmo Bio, CTB-LC3-2-IC). The secondary antibodies used were from Thermo Fisher Scientific (1:500, Alexa-conjugated anti-mouse, anti-goat, anti-human and anti-rabbit antisera) and Dabco (1:5,000, HRP-conjugated reagents). The purified LPS from *S*. Minnesota was from Adipogen (Ra (IAX-100-016), Rb (IAX-100-015), Rc (IAX-100-017), Rd1 (IAX-100-018), Rd2 (IAX-100-021), Re (IAX-100-021) and lipid A (IAX-100-001)).

Cell culture

HeLa cells were obtained from the European Collection of Authenticated Cell Cultures. Wild-type MEFs were provided by C. Sasakawa[36]. Cells were grown in IMDM supplemented with 10% FCS at 37 °C in 5% CO_2. All cell lines tested negative for *Mycoplasma*. Stable cell lines were generated by retroviral transduction or, for expression of different *Flag-GFP-RNF213* alleles, were generated using an inducible Piggybac transposon system[35]. In brief, *Rnf213*-knockout MEFs seeded in 24-well plates were transfected with 1 μg of PiggyBac plasmids[35] and 1 μg of pBase[37] using Lipofectamine 2000, and 2 days later cells were selected with puromycin. Protein expression was induced with 1 μg ml^{-1} doxycycline for at least 15 h in the presence or absence of 20 μM ZVAD.

RNA interference

HeLa cells were transfected with Silencer Select small interfering RNAs (siRNAs) against *RNF213* (Thermo Fisher Scientific, s33570 and s33660) or the nontargeting Silencer Select Negative Control (Thermo Fisher Scientific, No.1) using Lipofectamine RNAiMAX (Thermo Fisher Scientific). Experiments were performed three days after transfection.

Generation of knockout cells

To make *RNF213*- and *Rnf213*-knockout cells, oligonucleotides for the gRNA (mouse *Rnf213*: GAAGCGGTACATCATACGTG and human *RNF213*: GCTGAAAGCGGGCGCACTGC) were phosphorylated with T4 PNK (New England Biolabs) and cloned into pSpCas9(BB)-2A-GFP (Addgene, PX458). Subsequently, cells were transfected and the next day, GFP-positive single cells were sorted into a 96-well plate. Resulting HeLa clones were screened for lack of RNF213 expression by immunoblotting. Disruption of *RNF213* or *Rnf213* exons in HeLa and MEFs were verified by sequencing.

Bacteria

Escherichia coli strains MC1601 and NEB 10-beta were used for plasmid production and the BL21 strain was used for protein purification.

Salmonella enterica ser. Typhimurium strain 12023 and the isogenic Δ*rfaL* were provided by D. Holden.

To generate mutants in *S*. Typhimurium we used phage λ Red recombinase[38]. Mutants in *cptA, eptB*, *arnC* and *eptB* were generated in *S*. Typhimurium lacking rfaL. The following primers were used: *wzzB* forward (fwd) (CATTAATCCTATGGCATATATTTGCTTTATGGCTACACTGTCTCCAGCTTCATCCTTTTTTTAGTTAGGGTATCTATGGTGTAGGCTGGAGCTGCTTC); *wzzB* reverse (rev) (AAAAAACCGGGCAATGCCCGGTTTTTTAATGAGAAATTTTACCTGTCGTAGCCGACCACCATCCGGCAAAGAAGCTTACATATGAATATCCTCCTTAG); *fepE* fwd (GATAATTCTGACTTGCTGTTAGAATCTCTGACAGGAATGTGTTCTTTCATTGGATAAATTTTTCAGGTCATACGGCATGGTGTAGGCTGGAGCTGCTTC); *fepE* rev (GGTACCGCTGGGGCGGCGATAGTCGCCCACACTGATGACAAAGCCGGATATCGCTATCCGGCTTTTCGGGTAAATCACATATGAATATCCTCCTTAG); *rfc* fwd (TTTGCCTGATGGTAATATTTTTAATACTAAGCATTTTTTCTAAAGGCTCTATTGGTGTAGGCTGGAGCTGCTTC); *rfc* rev (ACAATTTTTACGCTTCAGAGCCAAATAAAACGGCGGCATTGCCGCCGTATAACTTACATATGAATATCCTCCTTAG); *cptA* fwd (TATCCGGACTACGGGAGAGAAGCACGCCAGGCCCGATAAGCGTTAGCGTTATCGGGCAACATACAGGATGGTGTAGGCTGGAGCTGCTTC); *cptA* rev (GTTTGCTTCAGATTCTTTTAAGGTTCAGGCGTTACGTTTGGCGCTACGATTAAAGACAGGCTCTCATTCTACATATGAATATCCTCCTTAG); *eptA* fwd (AAGTTCTTAAGGTTCACTTAATTTTACTTTGTCACGATTAGCGTCACCGAATCGATGGACGCATCAACATGGTGTAGGCTGGAGCTGCTTC); *eptA* rev (GCCTTCGGTTTGCGCGGCGAGTATTAACCCCTGTAATAATAGCGTGTCGTCTTCAACAATCAGTATCTTCACATATGAATATCCTCCTTAG); *arnC* fwd (CCGGACATGACCGAGAGTGACTTTGATCGAGTCATTACCGCCCTTCATCAGATAGCAGGACAATAAGCATGGTGTAGGCTGGAGCTGCTTC); *arnC* rev (ATACCCGGCATCCAGTACGGCCTGCACCCCCTGACATCCCATATCGTGATAGGCAAAAATAACGGCTTTCACATATGAATATCCTCCTTAG); *eptB* fwd (GCGTTAGCCGCATATTTACCTGTTTGATTAAAGAATCGTTGTACAGGTCGTTTTTATCCCGATTCCCAGGGTTTGTTTGCATGGTGTAGGCTGGAGCTGCTTC); *eptB* rev (CATCTTACTGCTCAGGCGCACGCCCGTCAATCCCTTAGTCGCAAAATACAATTCAATCGGCGAGAAAGTCGGCAGACAACCATATGAATATCCTCCTTAG); *rfaJ* fwd (GAAGCATTATACTTCGGGTATAAATTATTATATAGCCTACTTTAAACGTAAACTTCTTGAATAAAACCCATAGGTGATGTAATGGTGTAGGCTGGAGCTGCTTC); and *rfaJ* rev (TTTTCACCGTCTTTTTTGACAAAGACGGTATAGTTTTTAATCTTTTTTTCAATAATCATAATGGAGATTTAGGGAGGGGAACATATGAATATCCTCCTTAG).

Resistance cassettes were removed using Flp recombinase and genotypes were verified by sequencing.

Bacterial infections and extraction

The *S*. Typhimurium was grown overnight in Luria broth (LB) and subcultured (1:33) in fresh LB for 3.5 h before infection.

To enumerate intracellular bacteria, MEFs in 24-well plates were infected with 20 μl of 1:15 diluted sub-culture for 8 min at 37 °C. Following 2 washes with warm PBS and incubation in IMDM supplemented with 10% FCS and 100 μg ml^{-1} gentamycin for 2 h, cells were cultured in IMDM supplemented with 10% FCS and 20 μg ml^{-1} gentamycin. To determine intracellular *S*. Typhimurium colony-forming units (CFUs), cells from triplicate wells were lysed in 1 ml of cold PBS containing 0.1% Triton X-100. Serial dilutions were plated in duplicate on LB agar.

To extract bacteria from host cells for biochemical analysis, cells seeded in a 6-well plate were infected with 100 μl of undiluted subculture for 20–30 min at 37 °C. Cells were incubated in medium containing 100 μg ml^{-1} gentamycin, washed once with PBS and lysed in 1 ml ice cold PBS containing 0.1% Triton X-100. Lysates were centrifuged at 300*g* for 5 min at 4 °C and supernatant containing bacteria was collected and centrifuged at 16,100*g* for 10 min at 4 °C. The bacterial pellet was washed once with PBS, followed by bacterial lysis in 50 μl BugBuster (Merck) including 2 mM iodoacetamide for 5 min at room temperature. The BugBuster lysate was centrifuged at 16,100*g* for 10 min at room temperature, the supernatant was split up in 2 fractions: one was directly

mixed with Laemmli buffer (Bio-Rad) containing 100 mM DTT and boiled for 5 min; the other fraction (used to further purify ubiquitylated LPS) was heated at 90 °C for 15 min, centrifuged at 16,100*g* for 10 min at room temperature and this heat-cleared supernatant was mixed with Laemmli buffer containing 100 mM DTT. For mild alkaline hydrolysis of ubiquitylated LPS, samples were further incubated with 100 or 200 mM NaOH at 37 °C for 20 min. K48-linked di-ubiquitin (Boston Biochem) was used as an amide-linked control. Samples were boiled for 5 min and subjected to immunoblot analysis.

Immunoblot analysis

Post-nuclear supernatants from HeLa cells or MEFs were obtained following lysis with RIPA buffer (50 mM Tris pH7.4, 150 mM NaCl, 1% NP-40, 0.5% NaDOC, 0.1% SDS and 1× Halt protease inhibitor cocktail (Thermo Scientific)). Cleared supernatants were mixed with Laemmli buffer containing 100 mM DTT or 5% β-mercaptoethanol and samples were boiled for 5 min. Samples were run on NuPAGE 4–12% Bis-Tris gels (Thermo Fisher Scientific) in MES or MOPS SDS running buffer (Formedium) at 165 V for 45 min. An overnight wet transfer was used to transfer RNF213 protein onto methanol-activated PVDF membranes (Millipore). For other proteins, samples were transferred onto PVDF membranes using the Turbo transfer system (BioRad) for 7 min at 1.3 A. Membranes were blocked for 1 h in TBS-T (100 mM Tris pH 7.4, 150 mM NaCl, 0.1% Tween 20) containing 5% milk (Marvel), followed by overnight incubation with primary antibodies in TBS-T containing 5% milk. Membranes were washed in TBS-T, incubated with secondary HRP-conjugated antibodies (Dabco,1/5000) in TBS-T containing 5% milk followed by 3× 10-min TBS-T washes. In the case of FK2 staining, milk was replaced by 2% BSA throughout the whole procedure. Heat-cleared bacterial lysates were used to visualize ubiquitylated LPS with Flag or FK2 antibody; non-heat-cleared bacterial lysates were used to probe for GroEL as a loading control. Visualization following immunoblotting was performed using ECL detection reagents (Amersham Bioscience) and a ChemiDoc MP imaging system (BioRad).

LPS extraction and visualization

The *S*. Typhimurium strains were grown overnight at 37 °C in 2 ml of LB in a shaking incubator. Bacteria were centrifuged at 16,100*g* for 5 min, resuspended in 100 µl of SDS buffer (2% β-mercaptoethanol, 2% SDS and 10% glycerol, 50 mM Tris-HCl pH 6, 0.025% bromophenol blue) and incubated at 95 °C for 15 min. Ten µl of proteinase K (20 µg ml^{-1}, Qiagen) was added, and the samples were incubated for 3 h at 59 °C. Two hundred µl of ice-cold water-saturated phenol was added to each tube. Samples were then thoroughly vortexed and incubated at 65 °C for 15 min, vortexing an additional 2 to 3 times throughout. After cooling to room temperature, 1 ml of anhydrous diethyl ether was added to each tube. Samples were spun at 16,100*g* for 10 min in a cold centrifuge. The bottom blue layer was carefully extracted and mixed with 200 µl of ice-cold water saturated phenol. Once again, samples were incubated at 65 °C for 15 min before being mixed with 1 ml of diethyl ether. Tubes were centrifuged at 16,100*g* for 10 min and the bottom blue layer was extracted and combined with 150 µl of 2× SDS buffer. Samples were separated by SDS–PAGE and stained using the Pro-QTM Emerald 300 Stain Kit, according to the manufacturer's instructions. Stained gels were visualized using a ChemiDoc MP imaging system (Biorad).

Protein production in insect cells

pOP806_pACEBac1 2xStrep-RNF213-3xFLAG plasmid was transformed into DH10EmBacY (DH10Bac with YFP reporter). Blue–white screening was used to isolate colonies containing recombinant baculoviral shuttle vectors (bacmids) and bacmid DNA was extracted combining cell lysis and neutralisation using buffer P1, P2 and N3 (Qiagen) followed by isopropanol precipitation. A 6-well of Sf9 cells (Oxford Expression Technologies) grown at 27 °C in Insect-Xpress (Lonza) without shaking was transfected with bacmid plasmid using PEI transfection reagent. After 7 days, virus P1 was collected and used 1:100 to transduce 100 ml (1×10^6 cells per ml) Sf9 cells. After 7 days, virus P2 was collected. To express protein, 1 l Sf9 cells was transduced with 1:100 dilution of P2 virus and cells were incubated at 27 °C with 140 rpm shaking for 3 or 4 days. Cell pellets were snap-frozen and stored at −80 °C. To lyse cells, they were thawed in 50 mM HEPES, 200 mM KCl, 1 mM TCEP, pH 7.2 containing 1× universal nuclease (Pierce) and protease inhibitor tablets (Roche). The lysate was centrifuged at 20,000*g* for 30 min at 4 °C and cleared lysate was applied to a 5-ml StrepTrap HP column (GE Healthcare) and eluted with 50 mM HEPES, 200 mM KCl, 1 mM TCEP, containing 2.5 mM desthiobiotin pH 8. PD10 columns were used to buffer-exchange to 50 mM HEPES, 200 mM KCl and 0.25 mM TCEP, pH 7.2 and RNF213 protein (>1 mg ml^{-1}) was snap-frozen in liquid nitrogen and stored at −80 °C. All purification steps were carried out at 4 °C, using an ÄKTA pure 25 (GE Healthcare).

Protein production in *E. coli*

GST–RNF213 protein fragments were purified from BL21 (DE3)pLac1 cells that were transformed with pETM30 plasmids and grown overnight on TYE plates containing 50 µg ml^{-1} kanamycin. An overnight starter culture was diluted 1:1,000 in 1 l of LB containing 50 µg ml^{-1} kanamycin and grown at 37 °C at 220 rpm until an optical density at 600 nm of about 0.9 was reached. The flask was cooled to 16 °C and protein expression was induced overnight with 100 µM IPTG at 220 rpm at 16 °C. Cell pellets were resuspended in IVU reaction buffer containing 1.43 mM β-mercaptoethanol, 2 mg ml^{-1} DNaseI and EDTA-free protease inhibitor tablets. The suspension was homogenized using an EmulsiFlex-C3 (Avestin) for two passes at about 15,000 psi and cleared by centrifugation at 30,000 rpm for 30 min at 4 °C. The clarified lysate was applied to Amintra glutathione resin (Expedeon), washed with IVU reaction buffer containing 1.43 mM β-mercaptoethanol and eluted with IVU reaction buffer containing 1.43 mM β-mercaptoethanol and 20 mM glutathione, pH 8. Protein was buffer exchanged into 1× IVU buffer with 1 mM TCEP, snap-frozen and stored at −80 °C.

For the purification of His–UBE1, an N-terminal GST–ubiquitin fusion protein was expressed and lysed in β-mercaptoethanol-free lysis. The His–UBE1 β-mercaptoethanol-free clarified lysate was supplemented with 10 mM ATP and 10 $MgCl_2$ and incubated at room temperature for 30 min with Amintra glutathione resin (Expedeon), which were equilibrated with 50 mM Tris pH 8.5 and 2 mM ATP. The resin was then washed with DTT-free high salt buffer supplemented with 5 mM MgCl2. His–UBE1 was eluted in DTT-containing buffer and protein-containing fractions were applied to anion-exchange 6-ml Resource Q column (GE Healthcare) with a 0–25% linear gradient from buffer A (25 mM Tris pH 8.5, 10 mM DTT, 50 mM NaCl) to buffer B (25 mM Tris pH 8.5, 10 mM DTT, 1,000 mM NaCl) and size-exclusion chromatography (HiLoad 16/600 Superdex 75 pg, GE Healthcare) into buffer C (25 mM Tris pH 8.5, 10 mM DTT, 200 mM NaCl).

In vitro deubiquitylation reaction

A 15-cm dish of HeLa cells was infected with 100 µl Δ*rfc S*. Typhimurium for 30 min. At 4 h after infection, bacteria were extracted as described in 'Bacterial infections and extraction'. Bacterial pellets were washed and resuspended in DUB reaction buffer (50 mM Tris pH 7.5, 50 mM NaCl and 5 mM DTT) and incubated with USP2 catalytic domain (Boston Biochem) for 30 min at 37 °C.

In vitro ubiquitylation reaction

First, E2 was pre-charged in a 5× reaction by incubating 10 µM of UBCH5C or UBCH7 (Boston Biochem) in IVU reaction buffer (30 mM Hepes pH7.4, 100 mM NaCl, 10 mM $MgCl_2$) containing 50 mM ATP, 5 mM DTT, 200 µM Flag–ubiquitin (Boston Biochem) and 0.2 µM UBE1, for 15 min at 37 °C. Precharged E2 reaction was diluted to a 1× reaction with substrate (washed bacterial pellet obtained from a 10-cm dish of HeLa cells infected with *S*. Typhimurium for 4 h or purified LPS (Adipogen))

and E3 ligase (cell lysates or 350 nM recombinant RNF213). The reaction mix was incubated at 37 °C for 1 h, after which the reaction was centrifuged at 16,100*g* and the bacterial pellet or ubiquitylated LPS was washed twice in IVU reaction buffer containing 4 M urea. The bacterial pellet was lysed in BugBuster, the purified LPS solubilised in BugBuster and further processed for immunoblot analysis as previously described in 'Immunoblot analysis'.

Purification of E3 ligase activity for ubiquitylation of LPS

Suspension HeLa cells were used as a source for the unknown E3. HeLa lysate was dounce-homogenized in IVU reaction buffer containing 1 mM DTT and ultracentrifuged at 90,000 rpm in a TLA120.2 rotor. One ml of lysate was salted out using a 1–1.6 M $(NH_4)_2SO_4$ cut, which was applied to a butyl FF 1-ml column (GE Healthcare) in IVU reaction buffer containing 1 mM DTT and 1 M $(NH_4)_2SO_4$. The column was washed by reducing the salt concentration to 700 mM $(NH_4)_2SO_4$, and RNF213 activity was eluted by a further reduction to 0 mM $(NH_4)_2SO_4$. The enzymatic activity was enriched in the last step elution, this fraction was concentrated to 500 µl volume (vivaspin 2, 10,000 MWCO PES) and applied to a Superdex 200 10/300 column (GE Healthcare), equilibrated in IVU reaction buffer containing 1 mM DTT and 10% glycerol. The fractions with enzymatic activity were applied to a MonoS column and protein was gradient eluted (100 to 500 mM NaCl) using IVU reaction buffer containing 1 mM DTT and 10% glycerol. The eluted fractions were analysed by mass spectrometry. To assess activity, in vitro ubiquitylation reactions were performed using proteins fractions dialysed in IVU reaction buffer containing 1 mM DTT (Slide-A-Lyzer, Thermo Scientific, 69570).

Mass spectrometry

Fractions eluted from the MonoS column were prepared for mass spectrometric analysis by in solution enzymatic digestion. In brief, proteins were reduced in 10 mM DTT, and then alkylated with 55 mM iodoacetamide. After alkylation, proteins were digested with trypsin (Promega) overnight at 37 °C at an enzyme-to-protein ratio of 1:20. The resulting peptides were analysed by nano-scale capillary liquid chromatography with tandem mass spectrometry (LC–MS/MS) using an Ultimate U3000 HPLC (ThermoScientific Dionex) to deliver a flow of approximately 300 nl min^{-1}. A C18 Acclaim PepMap100 5 µm, 100 µm × 20 mm nanoViper (ThermoScientific Dionex), trapped the peptides before separation on a 25 cm PicoCHIP nanospray column packed with Reprosil-PUR C18 AQ (New Objective). Peptides were eluted with a 60-min gradient of acetonitrile (2% v/v to 80% v/v). The analytical column outlet was directly interfaced via a nano-flow electrospray ionization source, with a hybrid dual pressure linear ion trap mass spectrometer (Orbitrap Velos, ThermoScientific). Data-dependent analysis was carried out, using a resolution of 30,000 for the full mass spectrum, followed by ten tandem mass spectra in the linear ion trap. Mass spectra were collected over a m/z range of 300–2000. MS/MS scans were collected using a threshold energy of 35 for collision-induced dissociation. LC–MS/MS data were then searched against a protein database (UniProt KB) using the Mascot search engine programme (Matrix Science)[39]. Database search parameters were set with a precursor tolerance of 5 ppm and a fragment ion mass tolerance of 0.8 Da. Two missed enzyme cleavages were allowed and variable modifications for oxidized methionine, carbamidomethyl cysteine, pyroglutamic acid, phosphorylated serine, threonine and tyrosine were included. MS/MS data were validated using the Scaffold programme (Proteome Software)[40]. All data were additionally investigated manually.

Protein alignments

We identified animal homologues of human RNF213 from major animal lineages with human RNF213 as a query for iterative JACKHMMER[41] searches performed on combined UniProt and TrEMBL databases (with *e*-value cut-off = 0.001 and query length cut-off = 60%) and PSI-BLAST[42] searches on non-redundant database (with *e*-value cut-off = 0.001 and query length cut-off = 60%). We collected animal homologues of human RNF213 (that is, animal orthologues of human RNF213 and homologous RZ finger regions of human RNF213 and ZNFX1) and then we constructed multiple sequence alignments of orthologues and homologues using MSAPROBs[43], which were refined using HMMER profiles. These alignments were further manually corrected on the basis of Jalview[44] conservation scores. The logo was constructed using WebLogo[45].

Microscopy

Cells were grown on glass coverslips. After infection, cells were washed twice with PBS and fixed in 4% paraformaldehyde for 15 min. Cells were washed twice in PBS and then permeabilized in PBS with 0.1% Triton X-100 and blocked with PBS with 2% BSA. When staining for LC3, cells were permeabilized with 0.05% saponin in PBS with 2% BSA. Coverslips were incubated with primary antibodies followed by Alexa conjugated secondary antibodies in blocking solution for at least 1 h at room temperature. Coverslips were then mounted either in Prolong gold mounting medium or ProLong Gold Antifade Mountant (Invitrogen) for confocal imaging or super resolution microscopy, respectively.

Marker-positive bacteria were scored by eye on a Zeiss Axio Imager microscope using a 100×/1.4 NA Oil immersion lens, among at least 200 bacteria per coverslip.

Super-resolution images were acquired using an Elyra S1 structured illumination microscope (Carl Zeiss). The system has four laser excitation sources (405 nm, 488 nm, 561 nm and 640 nm) with fluorescence emission filter sets matched to these wavelengths. Structured illumination microscopy images were obtained using a ×63/1.4 NA oil immersion lens with grating projections at 3 rotations and 5 phases in accordance with the manufacturer's instructions. The number of *z* planes varied with sample thickness. Super-resolution images were calculated from the raw data using Zeiss ZEN software and plot profiles were made with FiJi ImageJ.

For live-cell resolution imaging, cells were seeded in 35-mm glass-bottom MatTek microwell dishes. After infection, cells were washed 4 times in warm PBS and incubated in Leibovitz's L-15 supplemented with 100 µg ml^{-1} gentamycin for the duration of the experiment. Images were acquired using a 100× super resolution Apo TIRF oil objective on a Nikon Eclipse Ti2 with a VisiTech iSIM high-speed super-resolution system. Movies were analysed using FiJi ImageJ.

Quantification and statistical analysis

All data were tested for statistical significance with Prism software (GraphPad Prism 8). The unpaired two-tailed Student's *t*-test was used to test whether two samples originated from the same population. Differences between more than two samples were tested using a one-way analysis of variance. Unless otherwise stated, all experiments were performed at least three times and the data were combined for presentation as mean ± s.e.m. All differences not specifically indicated as significant were not significant ($P > 0.05$). Significant values are indicated as $^{*}P < 0.05$ and $^{**}P < 0.01$. Statistical details, including sample sizes (n), are reported in the figures and figure legends.

For microscopy, when scoring marker-positive bacteria, at least three independent experiments with two technical replicates each were performed. Bacteria were scored by visual counting of $n > 200$ bacteria per replicate. Graphs show mean ± s.e.m.

When scoring intracellular CFUs, to score bacterial burdens, cells from triplicate wells were lysed and bacteria were plated in duplicate on LB agar. Each experiment was performed at least three times. Bacterial colonies were counted using the aCOLyte3 system (Synbiosis). Graphs show mean ± s.e.m.

Reporting summary

Further information on research design is available in the Nature Research Reporting Summary linked to this paper.

Data availability

All data are included in the Article and its Supplementary Information. Gel source images are provided in Supplementary Fig. 1. Materials can be obtained from the corresponding authors upon request. Source data are provided with this paper.

34. Randow, F. & Sale, J. E. Retroviral transduction of DT40. *Subcell. Biochem.* **40**, 383–386 (2006).
35. Glover, J. D. et al. A novel piggyBac transposon inducible expression system identifies a role for AKT signalling in primordial germ cell migration. *PLoS ONE* **8**, e77222 (2013).
36. Ogawa, M. et al. A Tecpr1-dependent selective autophagy pathway targets bacterial pathogens. *Cell Host Microbe* **9**, 376–389 (2011).
37. Yusa, K., Zhou, L., Li, M. A., Bradley, A. & Craig, N. L. A hyperactive piggyBac transposase for mammalian applications. *Proc. Natl Acad. Sci. USA* **108**, 1531–1536 (2011).
38. Datsenko, K. A. & Wanner, B. L. One-step inactivation of chromosomal genes in *Escherichia coli* K-12 using PCR products. *Proc. Natl Acad. Sci. USA* **97**, 6640–6645 (2000).
39. Perkins, D. N., Pappin, D. J. C., Creasy, D. M. & Cottrell, J. S. Probability-based protein identification by searching sequence databases using mass spectrometry data. *Electrophoresis* **20**, 3551–3567 (1999).
40. Keller, A., Nesvizhskii, A. I., Kolker, E. & Aebersold, R. Empirical statistical model to estimate the accuracy of peptide identifications made by MS/MS and database search. *Anal. Chem.* **74**, 5383–5392 (2002).
41. Johnson, L. S., Eddy, S. R. & Portugaly, E. Hidden Markov model speed heuristic and iterative HMM search procedure. *BMC Bioinformatics* **11**, 431 (2010).
42. Altschul, S. F. et al. Gapped BLAST and PSI-BLAST: a new generation of protein database search programs. *Nucleic Acids Res.* **25**, 3389–3402 (1997).
43. Liu, Y., Schmidt, B. & Maskell, D. L. MSAProbs: multiple sequence alignment based on pair hidden Markov models and partition function posterior probabilities. *Bioinformatics* **26**, 1958–1964 (2010).
44. Waterhouse, A. M., Procter, J. B., Martin, D. M. A., Clamp, M. & Barton, G. J. Jalview version 2—a multiple sequence alignment editor and analysis workbench. *Bioinformatics* **25**, 1189–1191 (2009).
45. Crooks, G. E., Hon, G., Chandonia, J.-M. & Brenner, S. E. WebLogo: a sequence logo generator. *Genome Res.* **14**, 1188–1190 (2004).

Acknowledgements We thank F. Begum, S. Peak Chew and M. Shekel of the LMB mass spectrometry facility for analysing samples; D. Morito for providing *RNF213* cDNA; and C. Gladkova and A. von der Malsburg for advice. This work was supported by a PhD fellowship from the Boehringer Ingelheim Trust to V.D., and by grants from the MRC (U105170648) and the Wellcome Trust (WT104752MA) to F.R.

Author contributions E.W. performed and analysed experiments that led to the discovery of LPS ubiquitylation. E.G.O. identified and characterized RNF213, with contributions from A.C.C. (super-resolution microscopy, and complementation and analysis of RNF213-knockout MEFs), K.B.B. (restriction of *Salmonella* by RNF213), C.P. (generation of *Salmonella* knockouts and analysis of RNF213-knockout MEFs), V.D. (validation of RNF213-knockout cells) and B.S. (bioinformatic analysis). E.G.O. and F.R. designed the study and wrote the manuscript.

Competing interests The authors declare no competing interests.

Additional information

Supplementary information The online version contains supplementary material available at https://doi.org/10.1038/s41586-021-03566-4.

Correspondence and requests for materials should be addressed to E.G.O. or F.R.

Peer review information *Nature* thanks Zhijian (James) Chen, J. Wade Harper and Samuel Miller for their contribution to the peer review of this work. Peer reviewer reports are available.

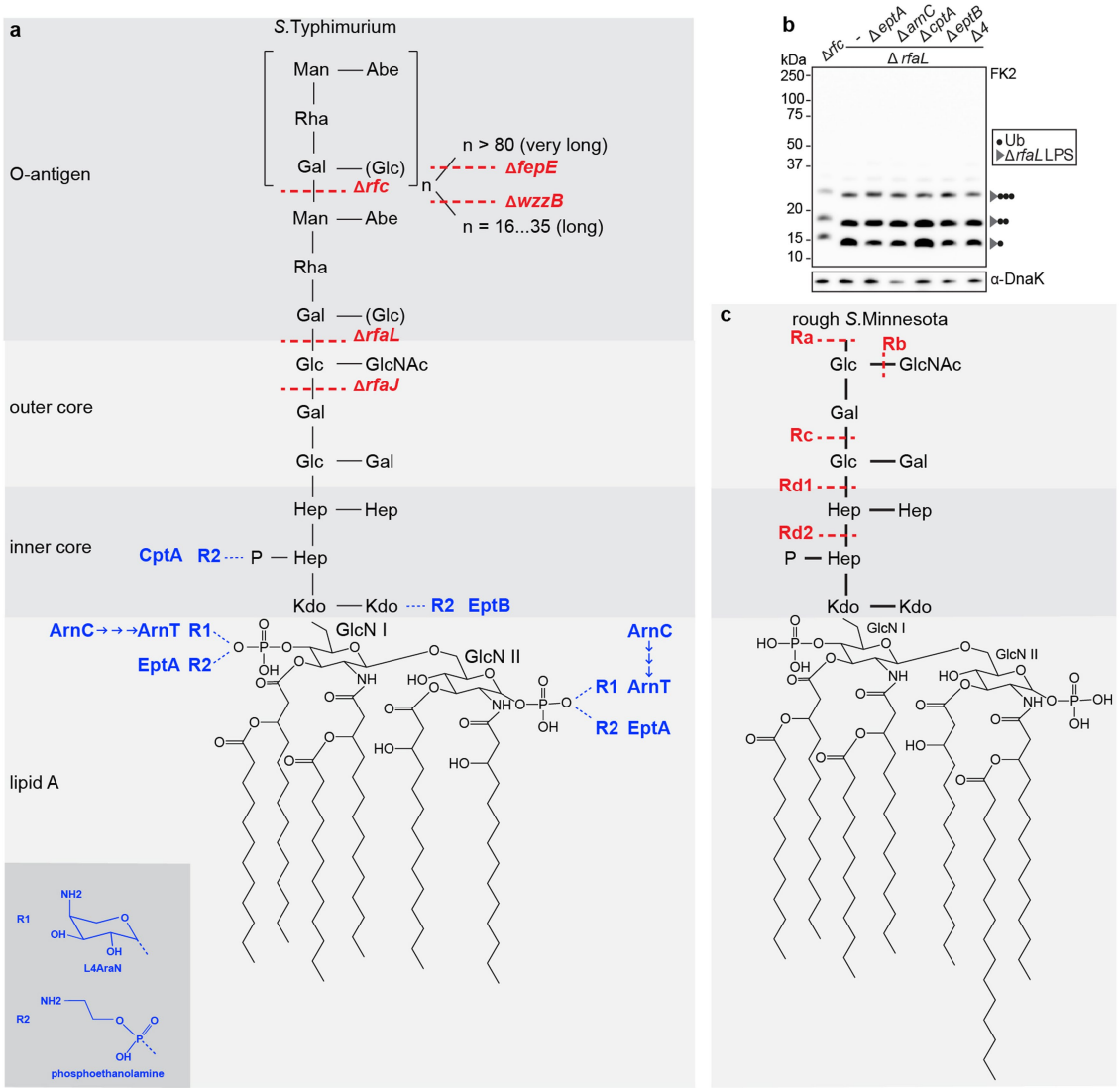

Extended Data Fig. 1 | LPS structure in *S.* Typhimurium and *S.* Minnesota. **a**, **c**, The composition of lipid A, inner core, outer core and O-antigen from *S.* Typhimurium (**a**) and rough variants of *S.* Minnesota (**c**). The *S.* Typhimurium mutants that are deficient in specific steps of LPS biosynthesis, and truncated LPS species from *S.* Minnesota, are indicated in red. Substoichiometric modifications introducing amino groups and the enzymes that are responsible are indicated in blue. ArnC (the undecaprenyl-phosphate 4-deoxy-4-formamido-L-arabinose transferase) functions upstream of ArnT and is required for the ultimate incorporation of L4AraN into LPS. EptA, EptB and CptA incorporate phosphoethanolamine into LPS. **b**, Immunoblot analysis of the indicated *S.* Typhimurium strains, extracted from HeLa cells. Blots were probed with the indicated antibodies. DnaK, loading controls for bacterial lysates. Δ4, Δ*eptA* Δ*arnC* Δ*cptA* Δ*eptB* in Δ*rfaL* background. Representative of three biological repeats. For gel source data, see Supplementary Fig. 1.

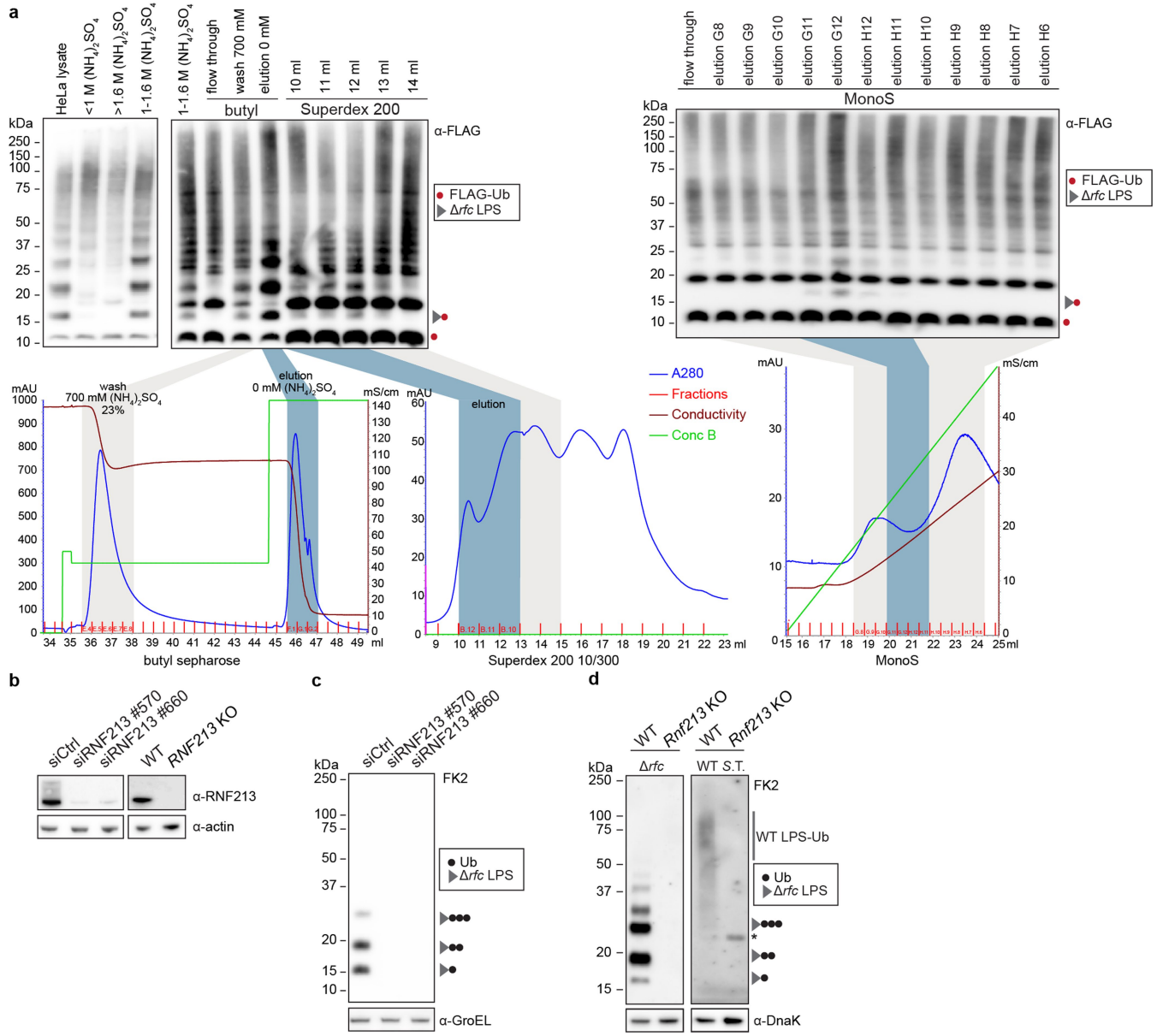

Extended Data Fig. 2 | RNF213 is required for ubiquitylation of LPS. **a**, In vitro ubiquitylation of *S.* Typhimurium Δ*rfc* extracted from infected HeLa cells. The reaction comprised Flag–ubiquitin, E1 enzyme (UBE1), E2 enzyme (UBCH5C) and fractionated HeLa cell lysate, as indicated. In the chromatograms depicted below each blot, light grey indicates fractions with little or no LPS-ubiquitylating activity, whereas blue indicates fractions with LPS-ubiquitylating activity used for further fractionation or mass spectrometry. **b**, Immunoblot analysis of HeLa cells transfected with the indicated siRNAs and wild-type HeLa and *RNF213*-knockout HeLa cells **c**, **d**, Immunoblot analysis of *S.* Typhimurium Δ*rfc* (**c**, **d** left) or wild type (**d** right) extracted from HeLa cells transfected with the indicated siRNAs (**c**) or extracted from wild-type or *Rnf213*-knockout MEFs (**d**). Representative of three biological repeats. Blots were probed with the indicated antibodies. Actin and GroEL or DnaK, loading controls for mammalian and bacterial lysates, respectively. Asterisk, non-specific band. For gel source data, see Supplementary Fig. 1.

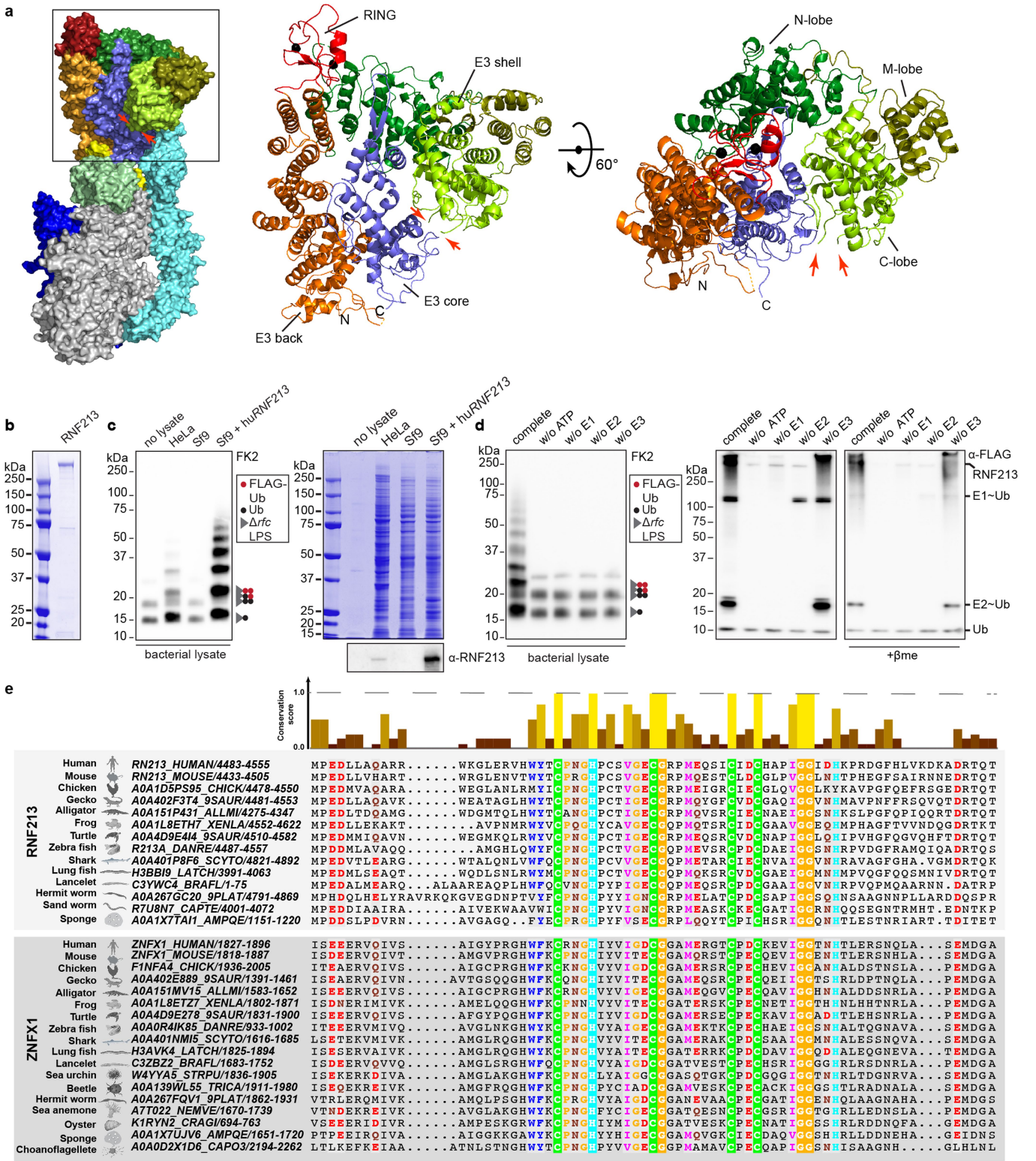

Extended Data Fig. 3 | Ubiquitylation of LPS by RNF213 is a RING-independent, RZ-finger-mediated reaction. a, RNF213 domain structure (Protein Data Bank 6TAX) (left) with domain colours corresponding to Fig. 3a, and zoom-in on the E3 module (middle, right) indicating N-terminal (N), middle (M) and C-terminal (C) lobes of the E3 shell domain. Red arrows point at the position of the unresolved RZ finger. **b**, Coomassie-stained gel of purified RNF213. **c**, **d**, Left panels show immunoblot analysis of *S.* Typhimurium Δ*rfc* extracted from HeLa cells and subjected to in vitro ubiquitylation using HeLa, Sf9 or Sf9 expressing human *RNF213* lysates (**c**) or purified RNF213 (**d**) corresponding to Fig. 3c, d. **c**, Right, Coomassie gel and immunoblot analysis of lysates used in Fig. 3c. **d**, Right, immunoblot analysis of in vitro ubiquitylation reaction supernatants, separated under non-reducing and reducing (+βme) conditions, corresponding to Fig. 3d. In **c**, **d**, blots were probed with indicated antibodies. **e**, Alignment and conservation scores of RZ fingers in RNF213 and ZNFX1 from the indicated species. Colour and height denote the degree of conservation (from Jalview) (top). RZ finger alignment (bottom). In **b**, **d**, representative shown of three biological repeats. In **c**, $n = 1$. For gel source data, see Supplementary Fig. 1.

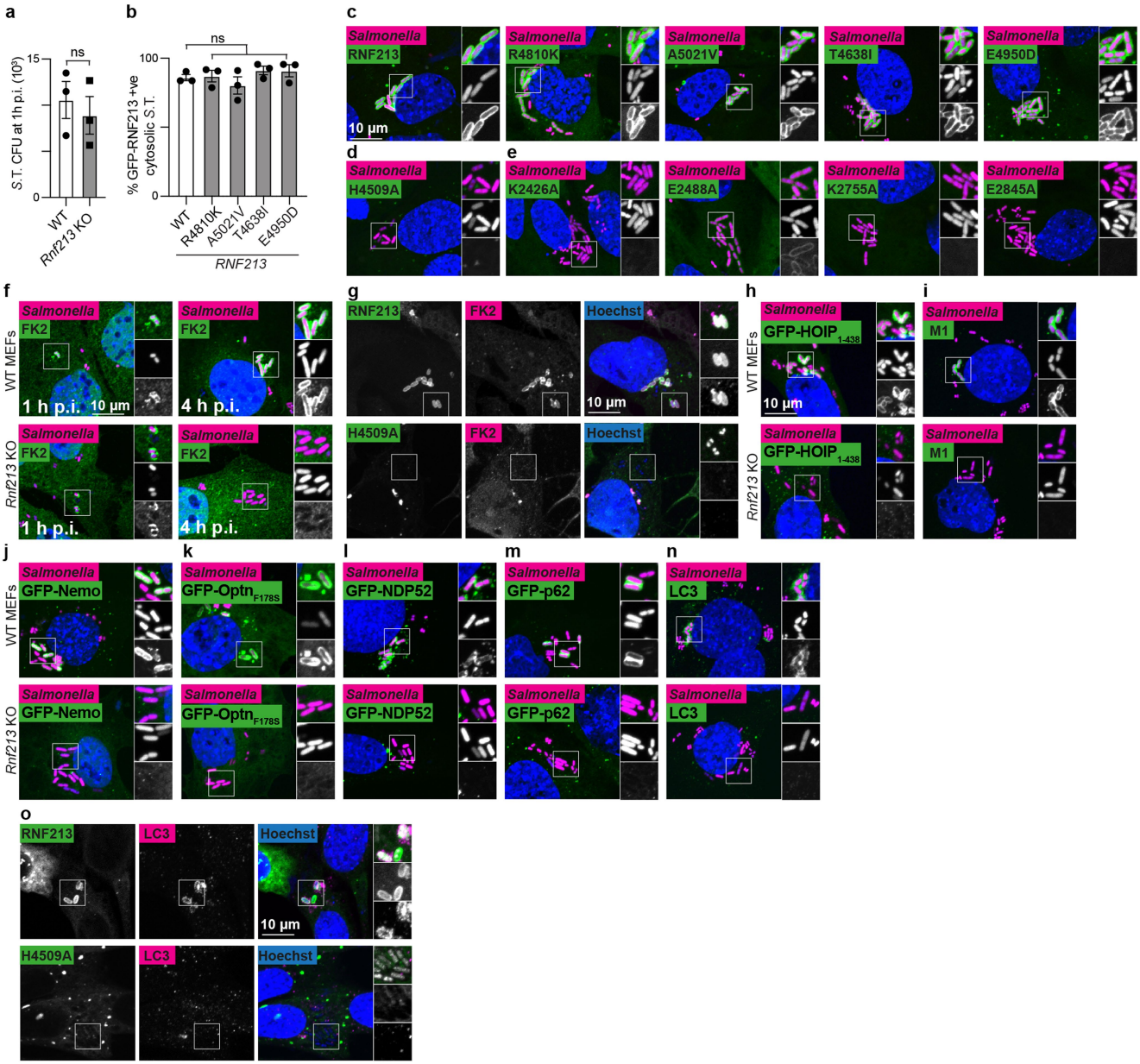

Extended Data Fig. 4 | RNF213 provides cell-autonomous immunity. a, CFU of *S.* Typhimurium at 1 h after infection, extracted from wild-type and *Rnf213*-knockout MEFs. Bacteria were counted by serial dilution of cell lysate on LB agar plates. Data are mean ± s.e.m. of three experiments. **b**, Percentage of cytosolic *S.* Typhimurium positive for Flag–GFP–RNF213 at 3 h after infection in *Rnf213*-knockout MEFs stably expressing the indicated *GFP-RNF213* alleles. **c**–**o**, Representative confocal micrographs for Fig. 4d–o. **c**–**e**, Wild-type or *Rnf213*-knockout MEFs stably expressing the indicated *GFP-RNF213* alleles infected with *mCherry*-expressing *S.* Typhimurium, fixed 3 h after infection. **f**–**o**, Wild-type and *Rnf213*-knockout MEFs (**f**, **g**, **n**), *Rnf213*-knockout MEFs stably expressing *GFP–RNF213*^{H4509A} (**g**, **o**) or wild-type and *Rnf213*-knockout MEFs stably expressing GFP–HOIP(1–438) or GFP–HOIP(1–438, T360A) (**h**), GFP–Nemo (**j**), GFP–optineurin(F178S) (**k**), GFP–NDP52 (**l**), GFP–p62 (**m**), infected with mCherry-expressing (**c**–**f**, **h**–**n**) or BFP-expressing (**g**, **o**) *S.* Typhimurium, fixed 3 h after infection and stained for FK2 (ubiquitin) (**f**, **g**), M1-linked linear ubiquitin chains (**i**) or LC3 (**n**, **o**). In **g**, **o**, for better visibility of bacteria, the Hoechst and BFP channel has been depicted in white in the zoomed sections. Scale bar, 10 µm (**c**–**n**). Statistical significance was assessed by two-tailed unpaired Student's *t*-test (**a**) or one-way analysis of variance (**b**). ns, not significant. Data are mean ± s.e.m. of three independent experiments (**a**, **b**) and micrographs are representative of three biological repeats (**c**–**o**).

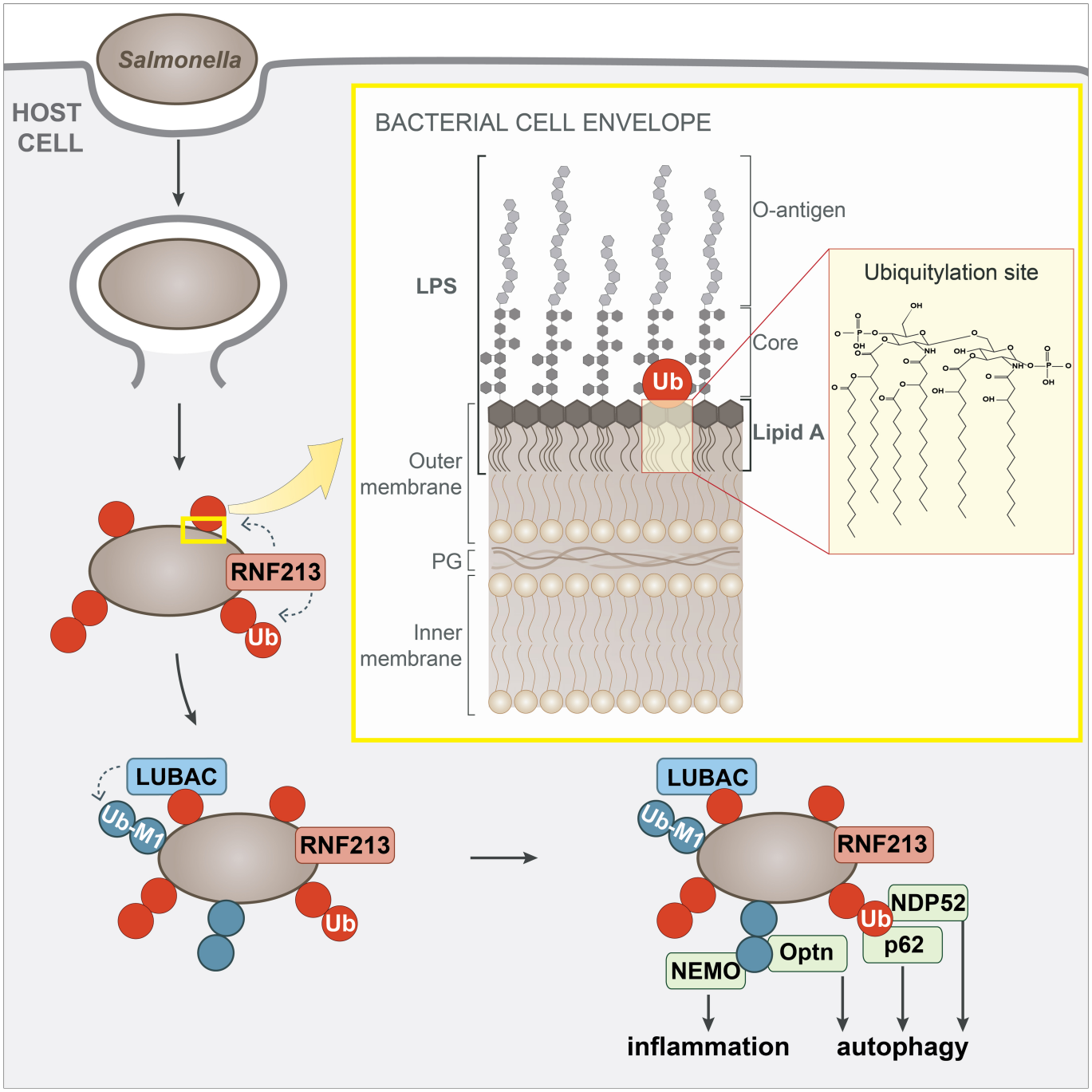

Extended Data Fig. 5 | Model of RNF213-mediated ubiquitylation of LPS during bacterial infection. Damage of *Salmonella*-containing vacuoles releases *S.* Typhimurium into the host cytosol, where RNF213 associates with the bacterial surface and ubiquitylates LPS, resulting in LUBAC recruitment and the deposition of M1-linked ubiquitin chains linked to an unidentified substrate. Recruitment of the autophagy cargo receptors NDP52 and p62 requires RNF213 but not LUBAC, while that of Optn and the IKK subunit NEMO relies on the activity of both RNF213 and LUBAC. Yellow insert, the structure of the Gram-negative cell envelope. PG, peptidoglycan. Red insert, lipid A, the minimal substrate for RNF213-mediated ubiquitylation of LPS. Ubiquitylation of lipid A is predicted to target its hydroxy or phosphate groups. The C6′ OH function is not available as a potential ubiquitylation site when the core is present.

nature research

Corresponding author(s): 2020-11-21099A, Elsje G. Otten and Felix Randow

Last updated by author(s): 12/04/2021

Reporting Summary

Nature Research wishes to improve the reproducibility of the work that we publish. This form provides structure for consistency and transparency in reporting. For further information on Nature Research policies, see our Editorial Policies and the Editorial Policy Checklist.

Statistics

For all statistical analyses, confirm that the following items are present in the figure legend, table legend, main text, or Methods section.

n/a	Confirmed	
☐	☒	The exact sample size (*n*) for each experimental group/condition, given as a discrete number and unit of measurement
☒	☐	A statement on whether measurements were taken from distinct samples or whether the same sample was measured repeatedly
☐	☒	The statistical test(s) used AND whether they are one- or two-sided *Only common tests should be described solely by name; describe more complex techniques in the Methods section.*
☒	☐	A description of all covariates tested
☒	☐	A description of any assumptions or corrections, such as tests of normality and adjustment for multiple comparisons
☐	☒	A full description of the statistical parameters including central tendency (e.g. means) or other basic estimates (e.g. regression coefficient) AND variation (e.g. standard deviation) or associated estimates of uncertainty (e.g. confidence intervals)
☐	☒	For null hypothesis testing, the test statistic (e.g. *F*, *t*, *r*) with confidence intervals, effect sizes, degrees of freedom and *P* value noted *Give P values as exact values whenever suitable.*
☒	☐	For Bayesian analysis, information on the choice of priors and Markov chain Monte Carlo settings
☒	☐	For hierarchical and complex designs, identification of the appropriate level for tests and full reporting of outcomes
☒	☐	Estimates of effect sizes (e.g. Cohen's *d*, Pearson's *r*), indicating how they were calculated

Our web collection on statistics for biologists contains articles on many of the points above.

Software and code

Policy information about availability of computer code

Data collection	Confocal images were taken on a Zeiss 780 microscope. Live imaging was performed on a Nikon Eclipse Ti2 equipped with a VisiTech iSIM super resolution confocal unit and a 100x/1.49 NA SR Apo TIRF objective LENS. Super resolution images were acquired using an Elyra S1 structured illumination microscope (Carl Zeiss Microscopy Ltd, Cambridge, UK).
Data analysis	Super-resolution images were calculated from the raw data using Zeiss ZEN software and plot profiles were made with FiJi ImageJ. All data were tested for statistical significance with Prism software (GraphPad Prism8). MS/MS data were validated using the Scaffold programme (Proteome Software Inc., USA)

For manuscripts utilizing custom algorithms or software that are central to the research but not yet described in published literature, software must be made available to editors and reviewers. We strongly encourage code deposition in a community repository (e.g. GitHub). See the Nature Research guidelines for submitting code & software for further information.

Data

Policy information about availability of data

All manuscripts must include a data availability statement. This statement should provide the following information, where applicable:

- Accession codes, unique identifiers, or web links for publicly available datasets
- A list of figures that have associated raw data
- A description of any restrictions on data availability

All data are included in the paper and its supplementary information files. For gel source images, see Supplementary Fig.1. Source data for graphs in Fig.2, Fig.4 and Exteded Data Fig. 4 are provided with this paper. Materials can be obtained from the corresponding authors upon request.

Field-specific reporting

Please select the one below that is the best fit for your research. If you are not sure, read the appropriate sections before making your selection.

☒ Life sciences ☐ Behavioural & social sciences ☐ Ecological, evolutionary & environmental sciences

For a reference copy of the document with all sections, see nature.com/documents/nr-reporting-summary-flat.pdf

Life sciences study design

All studies must disclose on these points even when the disclosure is negative.

Sample size	No statistical methods were used to predetermine sample size for experimentation. Given the minimal experimental variation in clonal cell lines, a minimum of three technical replicates were used per sample.
Data exclusions	No technical replicates were excluded.
Replication	Experiments shown in the manuscript were reliably reproducible. Number of independent biological repeats are stated in the figure legends.
Randomization	No randomization; all experiments were started from common pools of cells and bacteria.
Blinding	No blinding was applied, because phenotypes were very "black and white" revealing the sample identity.

Reporting for specific materials, systems and methods

We require information from authors about some types of materials, experimental systems and methods used in many studies. Here, indicate whether each material, system or method listed is relevant to your study. If you are not sure if a list item applies to your research, read the appropriate section before selecting a response.

Materials & experimental systems

n/a	Involved in the study
☐	☒ Antibodies
☐	☒ Eukaryotic cell lines
☒	☐ Palaeontology and archaeology
☒	☐ Animals and other organisms
☒	☐ Human research participants
☒	☐ Clinical data
☒	☐ Dual use research of concern

Methods

n/a	Involved in the study
☒	☐ ChIP-seq
☒	☐ Flow cytometry
☒	☐ MRI-based neuroimaging

Antibodies

Antibodies used	Primary antibodies used: FK2 (1:200,Enzo Life Science, BML-PW8810), anti-GroEL (1:1000, Enzo Life Science, ADI-SPS-875-F), anti-HA.11 (1:1000, Convance, MMS-101R), anti-actin (1:1000, Abcam, ab8227), anti-RNF213 (1:1000, Merck, HPA003347), anti-FLAG-M2-HRP (1:1000, Merck, A8592) and anti-GFP (1:1000, JL8, Clontech, 632381), anti-LPS (1:100, BioRad, 8210-0407), anti-Galectin 8 (1:100, R&D Systems, AF1305), anti-M1 (1:1000, 1F11/3F5/Y102L, GenenTech) and anti-LC3 (1:100, Cosmo Bio, CTB-LC3-2-IC). Secondary antibodies used: Thermo Fisher Scientific (1:500, Alexa-conjugated anti-mouse, anti-goat and anti-rabbit antisera) and Dabco (1:5000, HRP-conjugated reagents).
Validation	All antibodies were used according to manufacturers' instructions. Anti-RNF213 antibody was verified by knockdown and knockout of RNF213 (Extended Data Fig.2b).

Eukaryotic cell lines

Policy information about cell lines

Cell line source(s)	HeLa cells and mouse embryonic fibroblasts were obtained from ATCC
Authentication	Cell lines obtained directly from ATCC. No authentication was performed.
Mycoplasma contamination	All cells tested negative for mycoplasma.
Commonly misidentified lines (See ICLAC register)	No commonly misidentified cell line was used.